Supporting Information

A Dye-loaded Fe_4L_4 Cage for Efficient Photocatalytic C(sp^3)-H Activation

Junhao Zhang, Youpeng Shi, Yuchen Wu, Fengyu Yang, Xu Jing* and Chunying Duan

School of Chemistry, Dalian University of Technology, Dalian, 116024, China.

E-mail: xjing@dlut.edu.cn

Contents

1. Experimental Section.

Materials and methods:

All the chemicals and solvents were of reagent grade quality obtained from commercial sources and used without further purification.

Nuclear magnetic resonance:

^{1}H NMR spectra and ^{1}H NMR titration experiments were recorded on a Bruker AVANCE NEO 500 MHz spectrometer at 298 K, with chemical shifts (δ) reported in parts per million (ppm) relative to tetramethylsilane (TMS, δ = 0.0 ppm) as the internal standard. ^{1}H diffusion-ordered spectroscopy (^{1}H DOSY) measurements were performed on a Bruker AVANCE NEO 400 MHz spectrometer to confirm the formation of homogeneous host-guest assemblies in solution.

Liquid chromatography- mass spectra:

Electrospray ionization time-of-flight mass spectrometry (ESI-TOF-MS) was conducted on an Agilent G6224A HPLC-ESI-TOF/MS system using acetonitrile as the mobile phase, operating in positive-ion mode to characterize the molecular composition and charge state of the cage and host-guest complex.

Liquid UV-Vis spectra:

UV-Vis absorption spectra were measured on a Shimadzu UV 2600 UV-Vis spectrophotometer.

High-performance liquid chromatography:

HPLC was performed on a SHIMADZU LC-2030 Plus system equipped with a ZORBAX SB-C18 column (250 × 4.6 mm I.D, s-5 μm) using methanol/water as mobile phase, to determine catalytic reaction yields.

Fluorescence spectra.:

Fluorescence emission spectra were measured on an Edinburgh FLS1000

fluorescence spectrophotometer.

Single-Crystal X-ray diffraction

X-ray diffraction data were collected on a Bruker D8 Venture Photon II diffractometer with graphite-monochromated Ga-Kα radiation (λ = 1.34139 Å).

Synthesis procedures

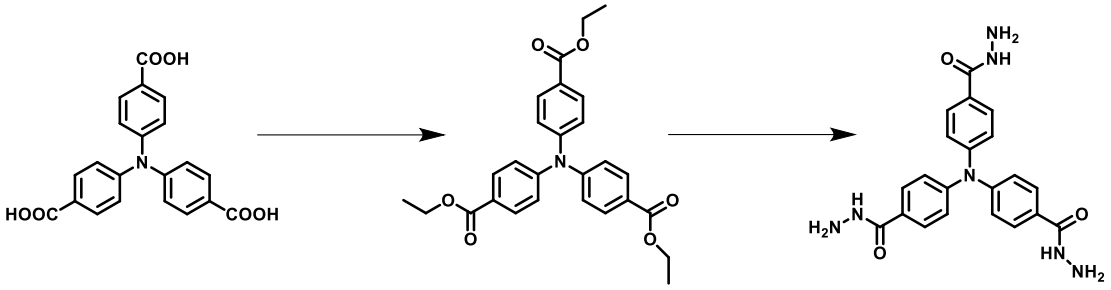

Figure S1 Synthesis of compound 4,4',4''-nitrilotri(benzohydrazide).

Synthesis of compound 4,4',4''-nitrilotri(benzohydrazide): 4,4',4''-nitrilotri(benzohydrazide) was synthesized by the method reported in the literature[1]. A suspension of 4,4',4''-nitrilotribenzoic acid (1.5 g, 3.98 mmol) in ethanol (35 mL) was cooled in an ice-water bath, and sulfuryl chloride (2 mL) was added dropwise. The resulting mixture was then heated under reflux for 12 h. A gray-white precipitate formed, which was collected by filtration and dried in an oven at 60 °C for 12 h to afford triethyl 4,4',4''-nitrilotribenzoate as a white solid. Yield: 84%.

Without further purification, the crude triethyl 4,4',4''-nitrilotribenzoate (1.54 g, 3.34 mmol) was dissolved in methanol (30 mL), and hydrazine hydrate (80 wt%, 7 mL) was added. The reaction mixture was heated under reflux for 96 h, during which a white precipitate was formed. The precipitate was collected by filtration, yielding 4,4',4''-nitrilotri(benzohydrazide) as a white solid Yield: 60%.**^{1}H NMR (500 MHz, DMSO-d$_6$)** δ 9.70 (s, 3H), 7.79 (d, *J* = 8.7 Hz, 6H), 7.07 (d, *J* = 8.7 Hz, 6H), 4.47 (s, 6H).

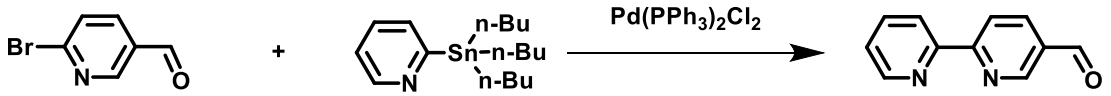

Figure S2 Synthesis of compound [2,2′-Bipyridine]-5-carboxaldehyde.

Synthesis of compound [2,2′-Bipyridine]-5-carboxaldehyde: 4,4',4''-nitrilotri(benzohydrazide) was synthesized by the method reported in the literature[2]. To a 250 mL round-bottom flask were added 6-bromonicotinaldehyde (2.79 g, 15.00

mmol), triphenylphosphine (0.39 g, 1.5 mmol), bis(triphenylphosphine)palladium(II) chloride (0.53 g, 0.75 mmol), and 2-(tributylstannyl)pyridine (4.80 mL, 15.00 mmol), followed by toluene (250 mL). The mixture was heated at reflux for 72 h under an argon-protected atmosphere, after which the resulting black solution was concentrated under reduced pressure. The crude residue was partitioned between dichloromethane (125 mL) and saturated aqueous ammonium chloride solution (75 mL). The organic layer was dried, filtered, and concentrated under reduced pressure. The crude product was first purified by silica gel column chromatography using a mixture of ethyl acetate (EA), dichloromethane (DCM), and petroleum ether (PE) (1:1:3, v/v/v) as the eluent. Removal of the solvent under reduced pressure afforded a pale yellow product. This material was further purified by a second silica gel column chromatography with an eluent system of EA/DCM/PE (1:2:1, v/v/v). The solvent was removed in vacuo to give the target compound as a white powder. Yield: 20%. **^{1}H NMR (500 MHz, $CDCl_3$)** δ 9.70 (s, 3H), 7.79 (d, *J* = 8.7 Hz, 6H), 7.07 (d, *J* = 8.7 Hz, 6H), 4.47 (s, 6H).

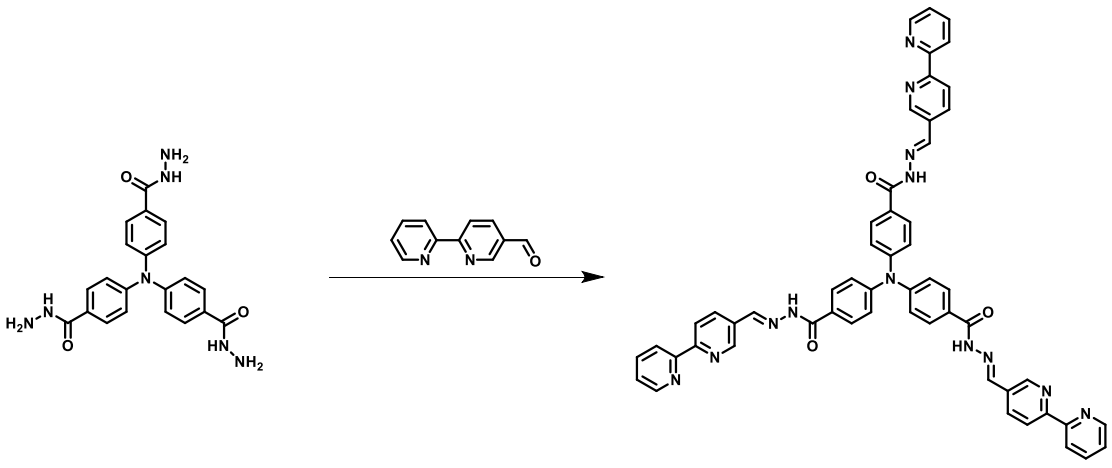

Figure S3 Synthesis of Compound L_1

Synthesis of Compound L_1: 8 drops of glacial acetic acid were added to a mixture of 4,4',4''-nitrilotri(benzohydrazide) (0.84 g, 2.00 mmol) and [2,2'-bipyridine]-5-carbaldehyde (1.11 g, 6.00 mmol) in 30 mL methanol. After the mixture was heated

under reflux conditions for 24 h, a bright yellow precipitate was formed and collected by filtration. Yield: 95%. **^{1}H NMR (500 MHz, DMSO-d$_6$)** δ 12.10 (s, 3H), 8.97 (s, 3H), 8.73 (d, *J* = 6.1 Hz, 3H), 8.58 (s, 3H), 8.50 (d, *J* = 8.4 Hz, 3H), 8.44 (d, *J* = 7.9 Hz, 3H), 8.33 (d, *J* = 10.4 Hz, 3H), 7.98 (d, *J* = 8.9 Hz, 9H), 7.52 – 7.48 (m, 3H), 7.26 (d, *J* = 8.7 Hz, 6H).

Synthesis of compound C$_1$: L$_1$ (91.8mg, 0.10mmol) and $Fe(ClO_4)_2·5H_2O$ (34.4mg, 0.10mmol) were stirred in DMSO solution under an argon-protected atmosphere at room temperature for 12 h. The reaction solution was subjected to recrystallization, yielding violet block-shaped crystals. Yield: 65%. **^{1}H NMR (DMSO-d$_6$, 500 MHz, ppm)** δ 12.14 (s, 3H), 8.90 (t, *J* = 9.2 Hz, 6H), 8.54 (d, *J* = 9.3 Hz, 3H), 8.30 (d, *J* = 7.5 Hz, 3H), 8.13 (s, 3H), 7.74 (d, *J* = 8.9 Hz, 6H), 7.63 (d, *J* = 6.6 Hz, 3H), 7.43 (d, *J* = 6.4 Hz, 3H), 7.30 (s, 3H), 7.10 (d, *J* = 8.9 Hz, 6H).

Synthesis of compound L$_2$: 8 drops of glacial acetic acid were added to a mixture of 4-(Dimethylamino)benzohydrazide (0.39 g, 2.00 mmol) and [2,2'-bipyridine]-5-carbaldehyde (0.37 g, 2.00 mmol) in 30 mL methanol. After the mixture was heated under reflux conditions for 24 h, a bright yellow precipitate was formed and collected by filtration. Yield: 96%. **^{1}H NMR (DMSO-d6, 500MHz, ppm)** δ 11.78 (s, 1H), 8.94 (d, J = 2.2 Hz, 1H), 8.72 (d, J = 4.8 Hz, 1H), 8.54 (s, 1H), 8.49 (d, J = 8.3 Hz, 1H), 8.44 (d, J = 7.9 Hz, 1H), 8.28 (d, J = 8.3 Hz, 1H), 8.01 – 7.95 (m, 1H), 7.85 (d, J = 9.0 Hz, 2H), 7.52 – 7.46 (m, 1H), 6.78 (d, J = 9.1 Hz, 2H), 3.02 (s, 6H).

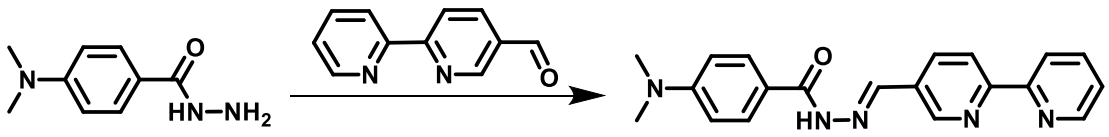

Figure S4 Synthesis of Compound L$_2$

Synthesis of compound M$_1$: L$_1$ (91.8mg, 0.10mmol) and $Fe(ClO_4)_2·5H_2O$ (34.4mg, 0.10mmol) were stirred in CH_3CN solution under argon protected atmosphere at room

temperature for 12 h. Excess diethyl ether was then added to the reaction solution to trigger precipitation. The resulting precipitate was collected by centrifugation, washed with diethyl ether three times, and dried under vacuum to afford a dark red solid product of **M1**. Yield: 73%.

General procedure for photocatalytic reactions

All catalytic reactions were carried out under a 395 nm LED. The reaction temperature was maintained at 298 K by circulating water through the outer jacket of the reactor.

The yields of the products were determined by HPLC analysis performed on SHIMADZU LC 2030 Plus analyzer using a ZORBAX SB-C18 reversed-phase column (250 × 4.6 mm I.D, s-5 μM) eluting with methanol/water to determine the yields of the catalytic reactions.

Reaction conditions. Substrates (0.10 mmol), C_{AQ} (0.50 μmol) in a mixed solution containing 1 mL of DMSO and 3 mL of CH_3CN under irradiation with a 395 nm LED under an O_2 atmosphere. Reaction time: 4 h for substrate **1a** (phthalan) and 8 h for other substrates.

The equations and the derivation[3]

Michaelis-Menten Equation. Michaelis-Menten equation was used to verify the mimic enzyme catalytic system.

$$V = V_{Max}\frac{[S]}{K_m + [S]}$$

Of which, V, the initial reaction rate of the enzymatic reactions; V_{max}, the maximum reaction rate of the enzymatic reactions; K_m, the Michaelis-Menten constant; [S], the concentration of the substrates. The equation could also transform into other form, like double-reciprocal plot showing below:

$$\frac{1}{V} = \frac{K_m}{V_{max}}\frac{1}{[S]} + \frac{1}{V_{max}}$$

For the nonlinear fitting of the host-guest complex system

For a 1:1 encapsulation process:

$$H + G \rightleftharpoons HG$$

Here, *H* represents the host in the system, *G* represents the guest, and *HG* represents the host–guest inclusion complex formed in the system.

$$[HG] = K_a[H][G] = K_a([H]_0 - [HG])([G]_0 - [HG])$$

Here, K_a denotes the association constant for the formation of the host–guest inclusion complex in the system, *[H]* denotes the concentration of the host, *[G]* denotes the concentration of the guest, and *[HG]* denotes the concentration of the host–guest inclusion complex formed.

Rearranging the equation gives:

$$[HG]^2 - \left([H]_0 + [G]_0 + \frac{1}{K_a}\right)[HG] + [H]_0[G]_0 = 0$$

The solution to this quadratic equation is:

$$[HG] = \frac{\left([H]_0 + [G]_0 + \frac{1}{K_a}\right) - \sqrt{\left([H]_0 + [G]_0 + \frac{1}{K_a}\right)^2 - 4[H]_0[G]_0}}{2}$$

For the UV–Vis absorption or fluorescence spectra obtained from titration of the host–guest complex in the system, a signal exists at any given point such that:

$$y = a[HG] + b[H] + c[G] = (a - b - c)[HG] + b[H]_0 + c[G]_0$$

Here, **a**, **b**, and **c** are specific constants.

$$y = (a - b - c)\frac{\left([H]_0 + [G]_0 + \frac{1}{K_a}\right) - \sqrt{\left([H]_0 + [G]_0 + \frac{1}{K_a}\right)^2 - 4[H]_0[G]_0}}{2} + b[H]_0 + c[G]_0$$

The relationship between the titration signal **y** and the initial concentration of the guest added to the system, $\mathbf{[G]_0}$, can be fitted using this equation.

In general, since the guest usually shows no response at the corresponding signal position (e.g., no fluorescence response or no absorption in the visible region), the equation can be simplified to:

$$y = a[HG] + b[H] = (a - b)[HG] + b[H]_0$$

$$y = (a - b)\frac{\left([H]_0 + [G]_0 + \frac{1}{K_a}\right) - \sqrt{\left([H]_0 + [G]_0 + \frac{1}{K_a}\right)^2 - 4[H]_0[G]_0}}{2} + b[H]_0$$

Let $k = (a - b)$, $y_0 = b[H]_0$

$$y = k\frac{\left([H]_0 + [G]_0 + \frac{1}{K_a}\right) - \sqrt{\left([H]_0 + [G]_0 + \frac{1}{K_a}\right)^2 - 4[H]_0[G]_0}}{2} + y_0$$

This equation is the nonlinear fitting relationship between the titration signal **y** and the initial concentration of the guest added to the system, $\mathbf{[G]_0}$, for the titration of a 1:1 host–guest inclusion complex.

2. Single Crystal X-ray Crystallography

Intensities of **C_1** were collected on a Bruker SMART APEX CCD diffractometer equipped with a graphite-monochromated and Ga-Kα (λ = 1.34139 Å) radiation source; the data were acquired using the SMART and SAINT programs[4, 5]. The structures were solved by direct methods and refined on F^2 by full-matrix least-squares methods using the SHELXTL version 5.1 software[6]. In the structural refinement of **C_1**, all the non-hydrogen atoms were refined anisotropically. Hydrogen atoms within the ligand backbones are allowed to ride on the parent nonhydrogen atoms. The SQUEEZE routine in the PLATON program was applied [7].

Compound	**C_1**
Empirical formula	$C_{348.5}H_{478.5}Cl_8Fe_4N_{69.5}O_{81.5}$
Formula weight	7452.48
Temperature [K]	150
Crystal system	Monoclinic
Space group (number)	C2/c (15)
a [Å]	61.956 (3)
b [Å]	43.506 (2)
c [Å]	46.899 (4)
α [°]	90
β [°]	125.4658 (13)
γ [°]	90
Volume [$Å^3$]	102957 (10)
Z	8
ρ_{calc} [gcm^{-3}]	0.962
μ [mm^{-1}]	1.222
F(000)	31584.0
Crystal size [mm^3]	0.12×0.12×0.12
Radiation	GaK_α (λ=1.34139 Å)
2θ range [°]	2.332 to 105.964
Index ranges	$-73 \leq h \leq 73$
	$-51 \leq k \leq 51$
	$-54 \leq l \leq 55$
Reflections collected	540417
Independent reflections	89997 [R_{int} = 0.1514 R_{sigma} = 0.0418]
Data / Restraints / Parameters	89997 / 4594 / 2719
Absorption correction T_{min}/T_{max}	0.850 / 0.850
(method)	(none)
Goodness-of-fit on F^2	1.061
Final *R* indexes	R_1 = 0.1256
[$I \geq 2\sigma(I)$]	wR_2 = 0.2262
Final *R* indexes	R_1 = 0.1640
[all data]	wR_2 = 0.2436
Largest peak/hole [$eÅ^{-3}$]	0.32/−0.37
CCDC number	2539665

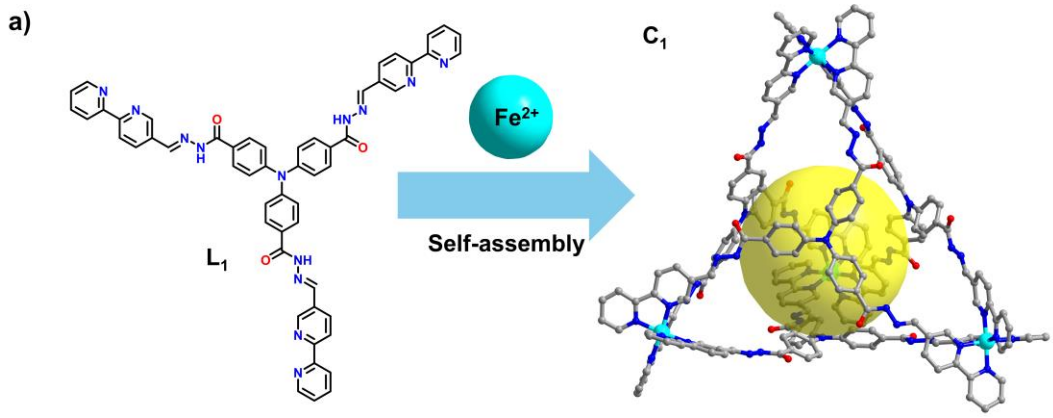

Figure S5. The self-assembly process of **C**$_1$ and the inner cavity (yellow balls), where iron, nitrogen, oxygen and carbon atoms are shown in pale blue, blue, red and grey respectively.

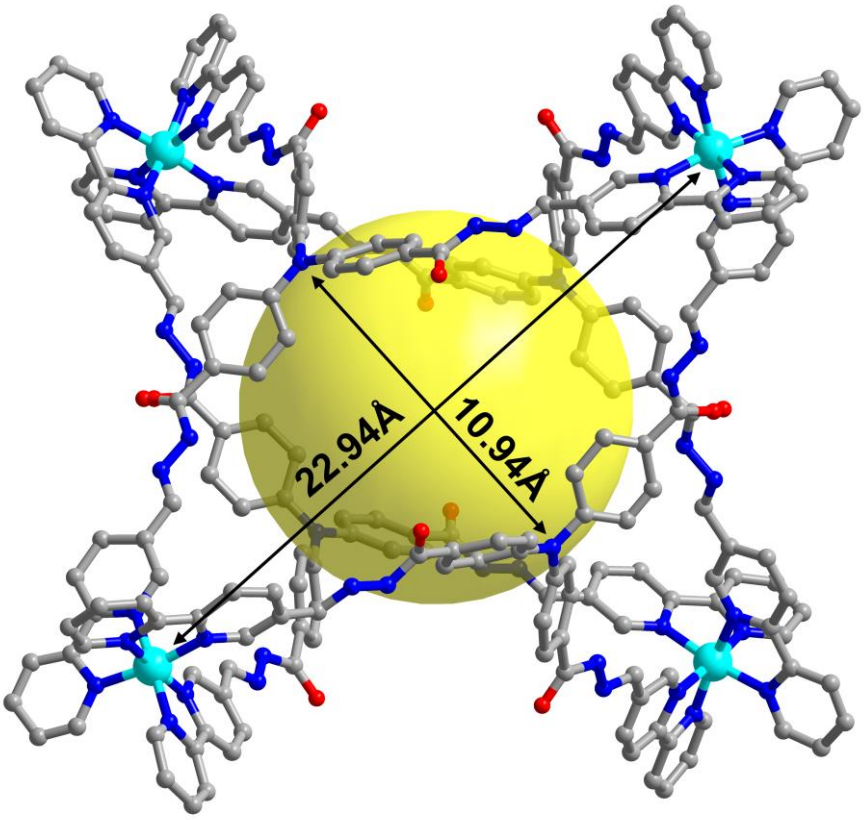

Figure S6. The openings of **C**$_1$, with an average Fe-Fe distance of about 22.9±0.6 Å and a maximum width of about 10.9±0.7 Å.

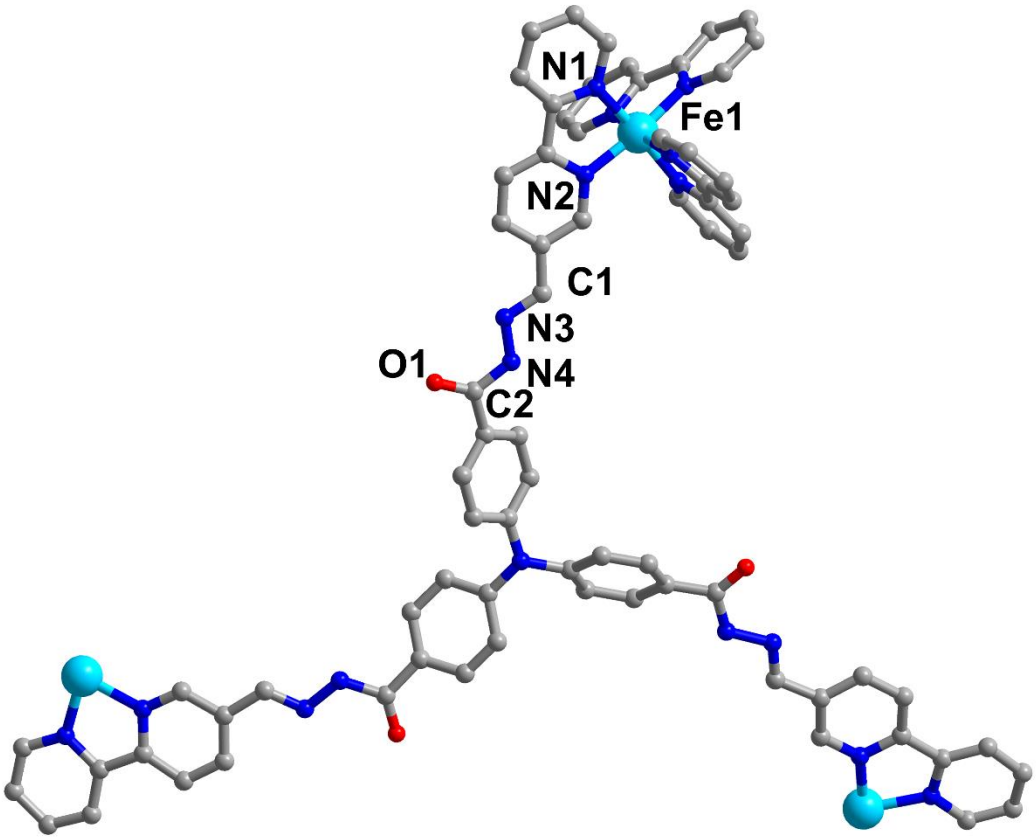

Figure S7. Molecular structure of $\mathbf{H_1}$ within a unique asymmetric unit, showing the backbone of the ligand in the complex. Selected bond distances (Å): Fe1-N1 1.976(4), Fe1-N2 1.967(5), N3-N4 1.391(5), N3-C1 1.281(5), N4-C2 1.372(5), C2-O1 1.219(5).

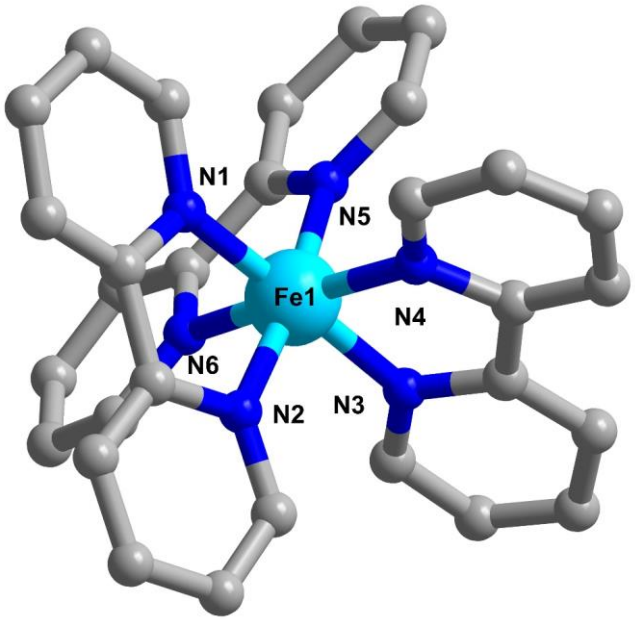

Figure S8. Coordination geometry of the Fe atom in **C**$_1$. Selected angles (°): N1-Fe1-N2 81.461(8), N1-Fe1-N3 175.5(2), N1-Fe1-N4 95.71(19), N1-Fe1-N5 95.0(2), N1-Fe1-N6 90.94(19), N2-Fe1-N3 95.1(2), N2-Fe1-N4 91.7(2), N2-Fe1-N5 172.92(19), N2-Fe1-N6 93.02(18), N3-Fe1-N4 81.401(8), N3-Fe1-N5 88.8(2), N3-Fe1-N6 92.18(19), N4-Fe1-N5 94.7(2), N4-Fe1-N6 172.34(19), N5-Fe1-N6 80.89(19)

3. Experimental Details.

^{1}H NMR spectra.

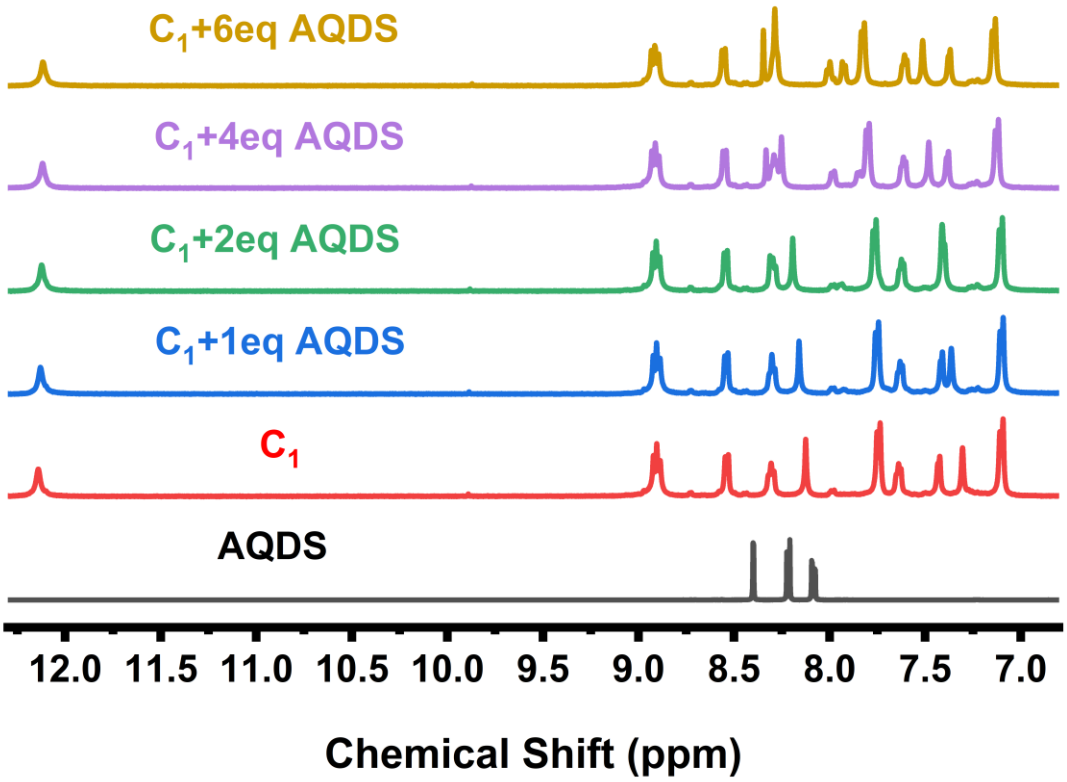

Figure S9 H-NMR titration spectra of the cage **C_1** upon addition of AQDS (500MHz, DMSO-d_6, 298K)

ESI-MS spectra.

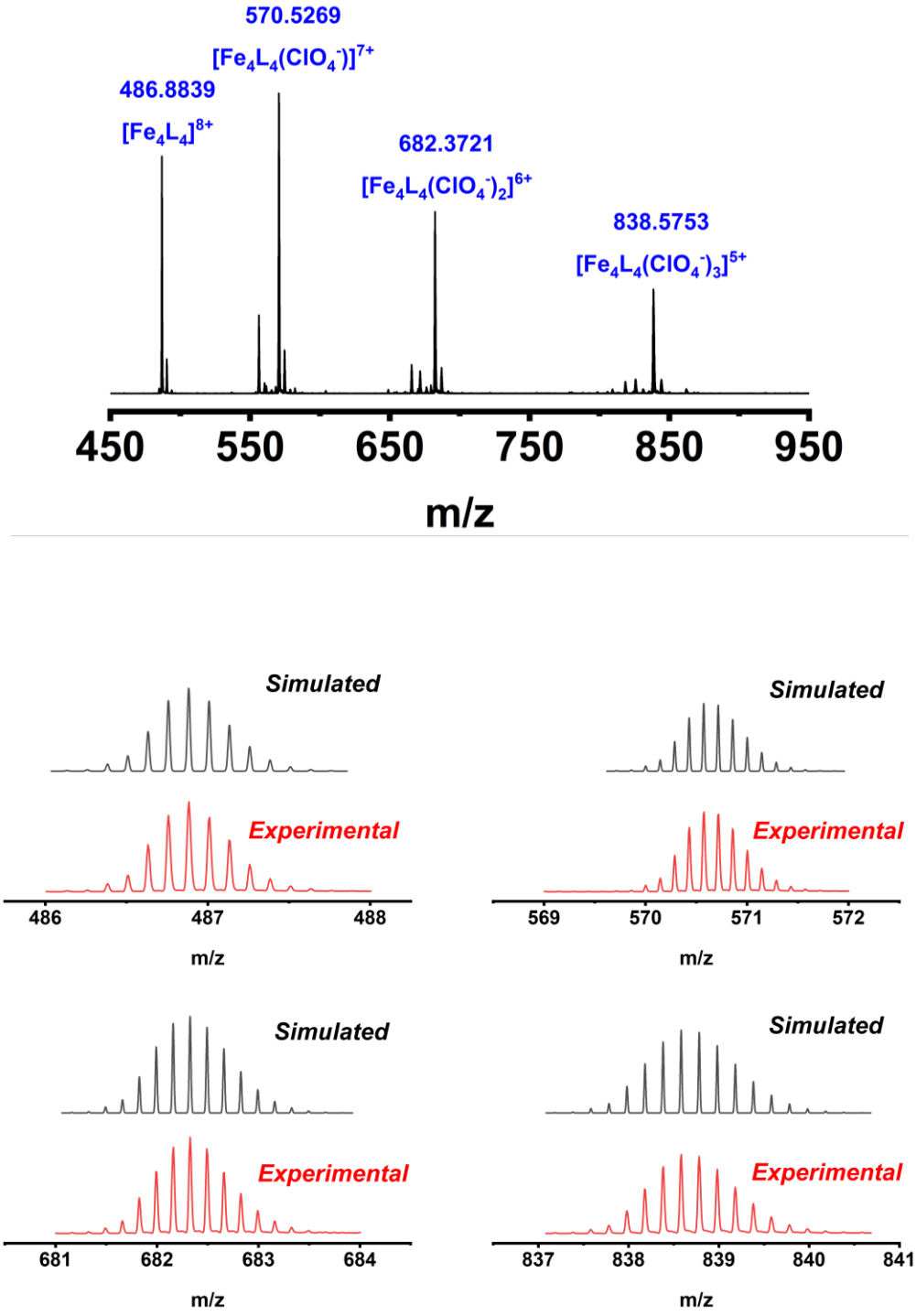

Figure S10. ESI-MS spectra of **C1** (0.1mM) in DMSO/CH_3CN (v: v=1: 3) solution.

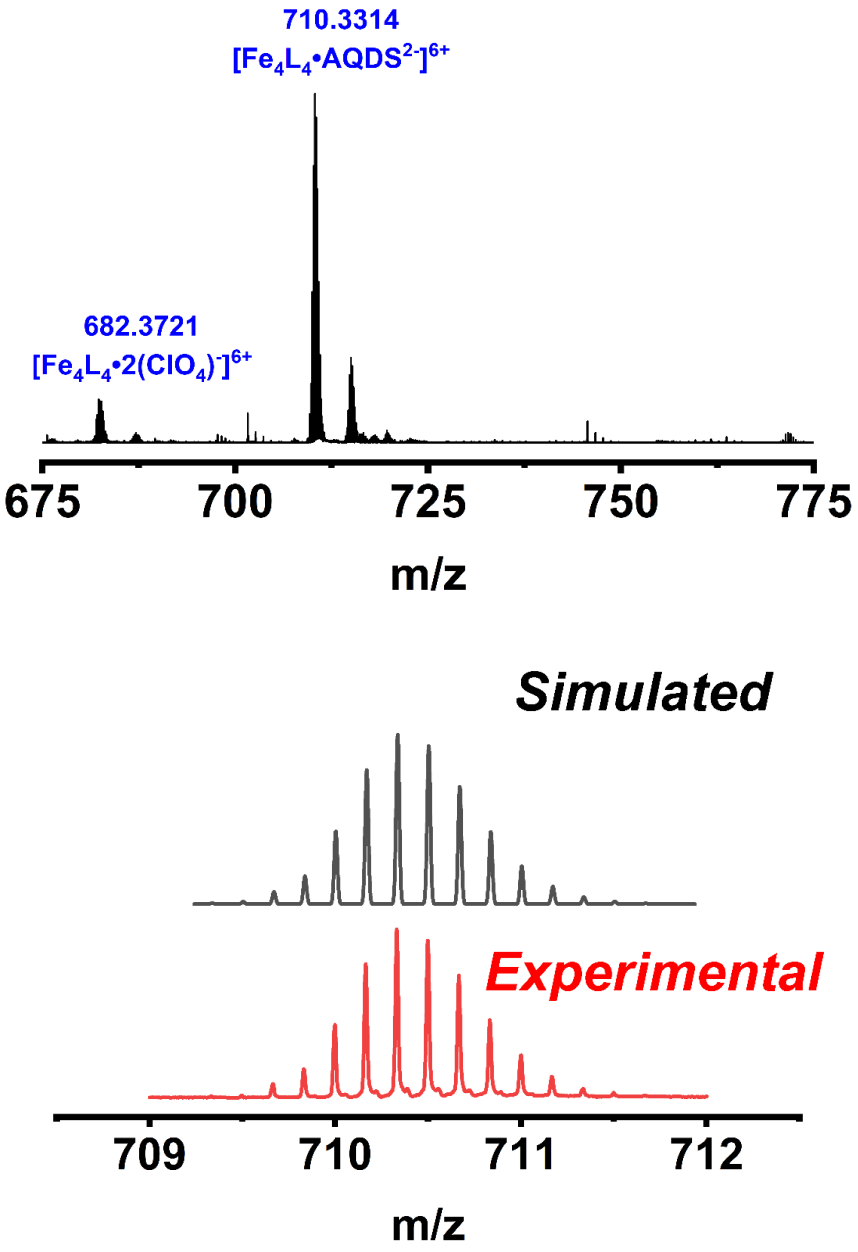

Figure S11. ESI-MS spectra of the mixture of **C**$_1$ (0.1 mM) and AQDS (0.2 mM) in DMSO/CH_3CN (v: v=1: 1) solution.

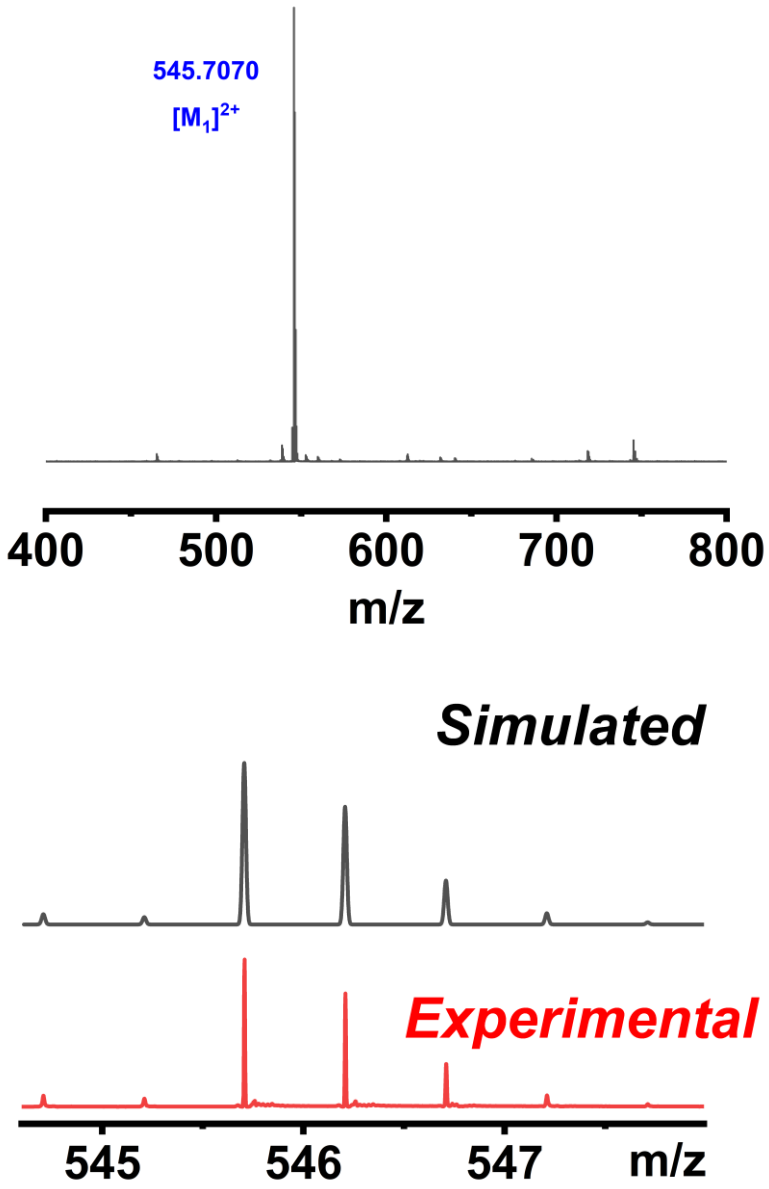

Figure S12. ESI-MS spectra of the mixture of **M1** (0.1 mM) in CH_3CN solution.

UV-Vis spectra

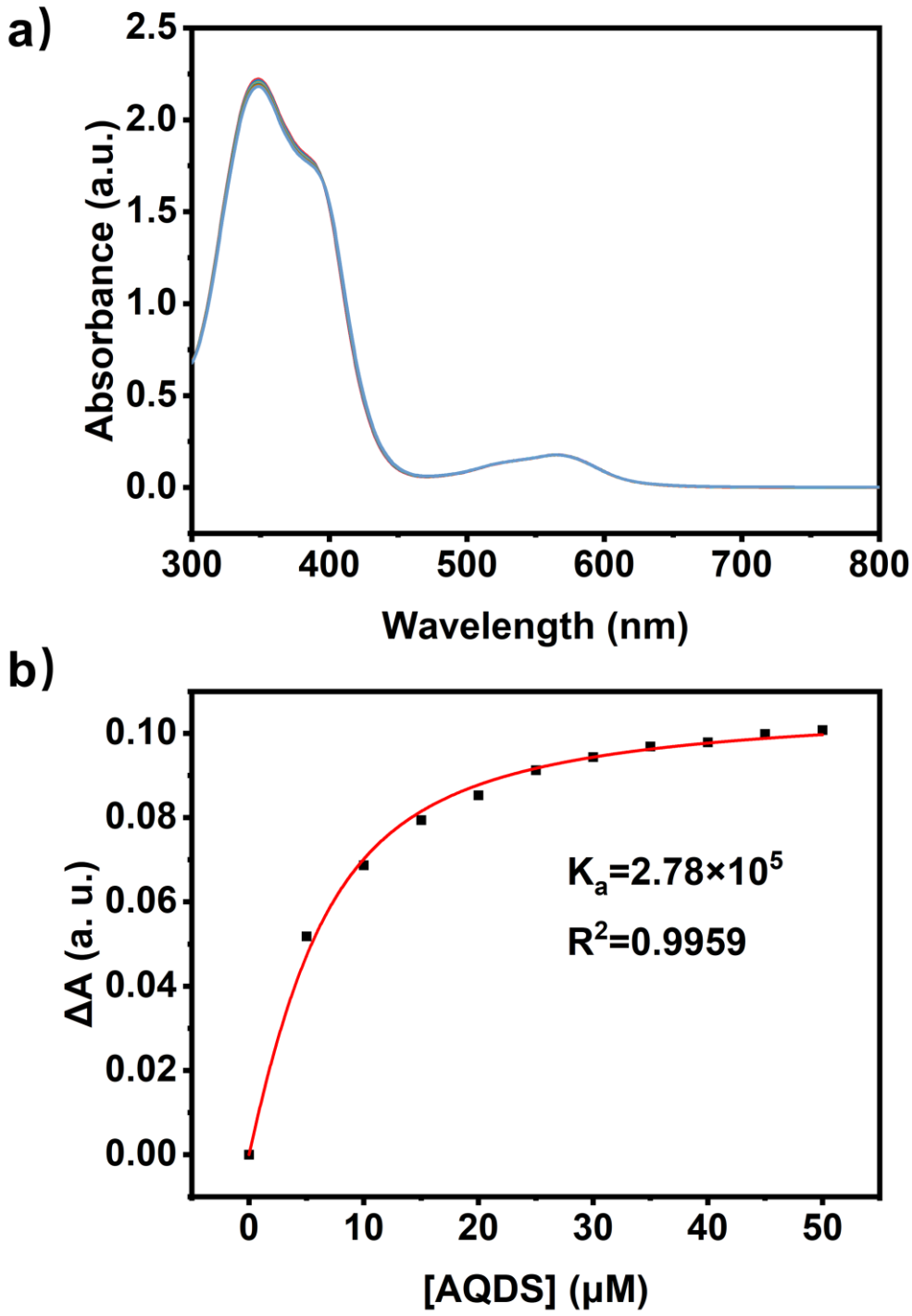

Figure S13. (a) UV-Vis spectra of the **C**$_1$ (0.005 mM) upon the addition of AQDS in an DMSO solution. (b) The nonlinear fitting of the titration curve (recorded absorption at 411 nm), showing a 1:1 host-guest binding stoichiometry between **C**$_1$ and AQDS with an association constant calculated as 2.78×10^5 M^{-1}.

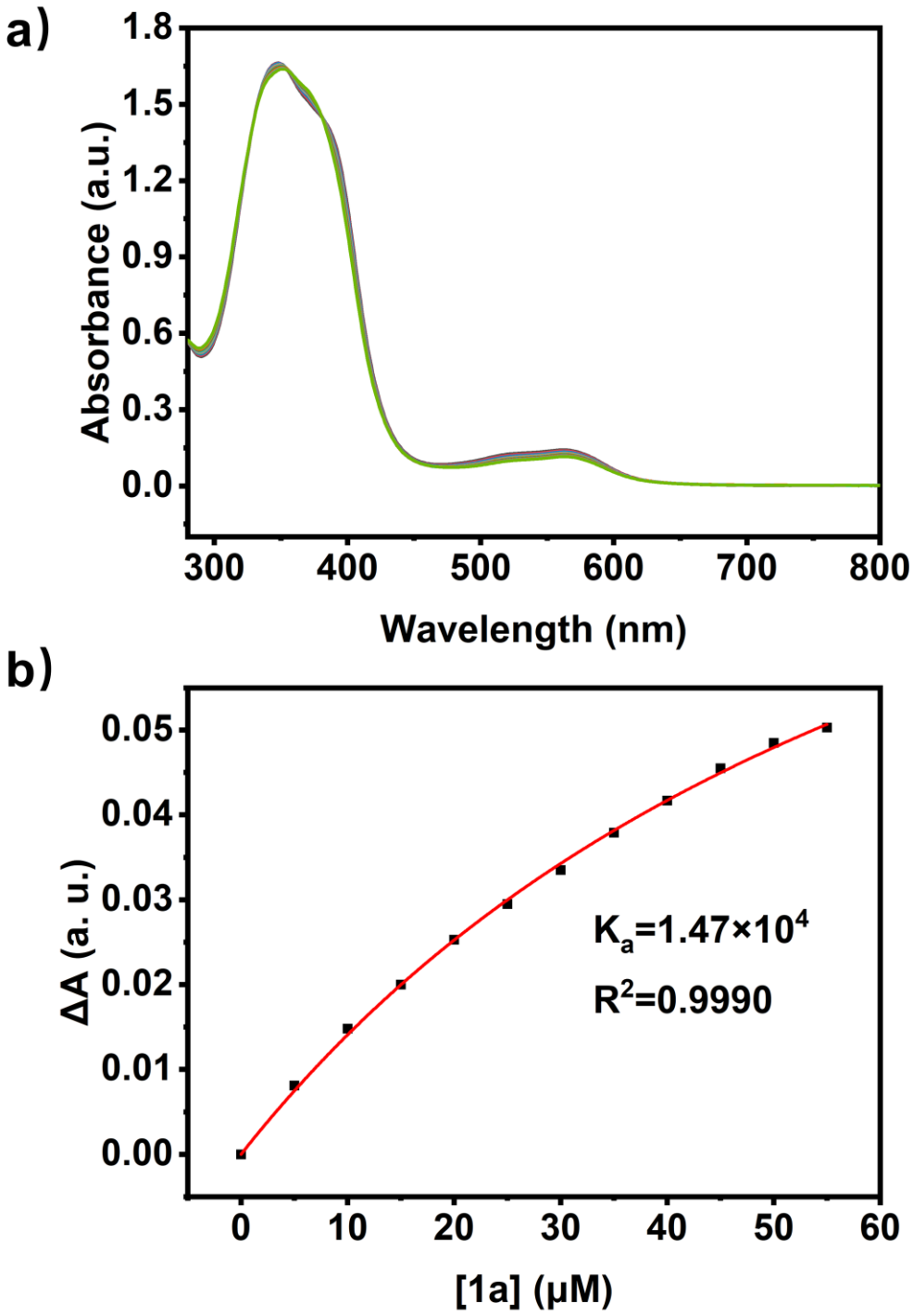

Figure S14. (a) UV-Vis spectra of the $\mathbf{C_1}$ (0.005 mM) upon the addition of **1a** in a DMSO solution. (b) The nonlinear fitting of the titration curve (recorded absorption at 305 nm), showing a 1:1 host-guest binding stoichiometry between $\mathbf{C_1}$ and **1a** with an association constant calculated as 1.47×10^4 M^{-1}.

Luminescence Spectra

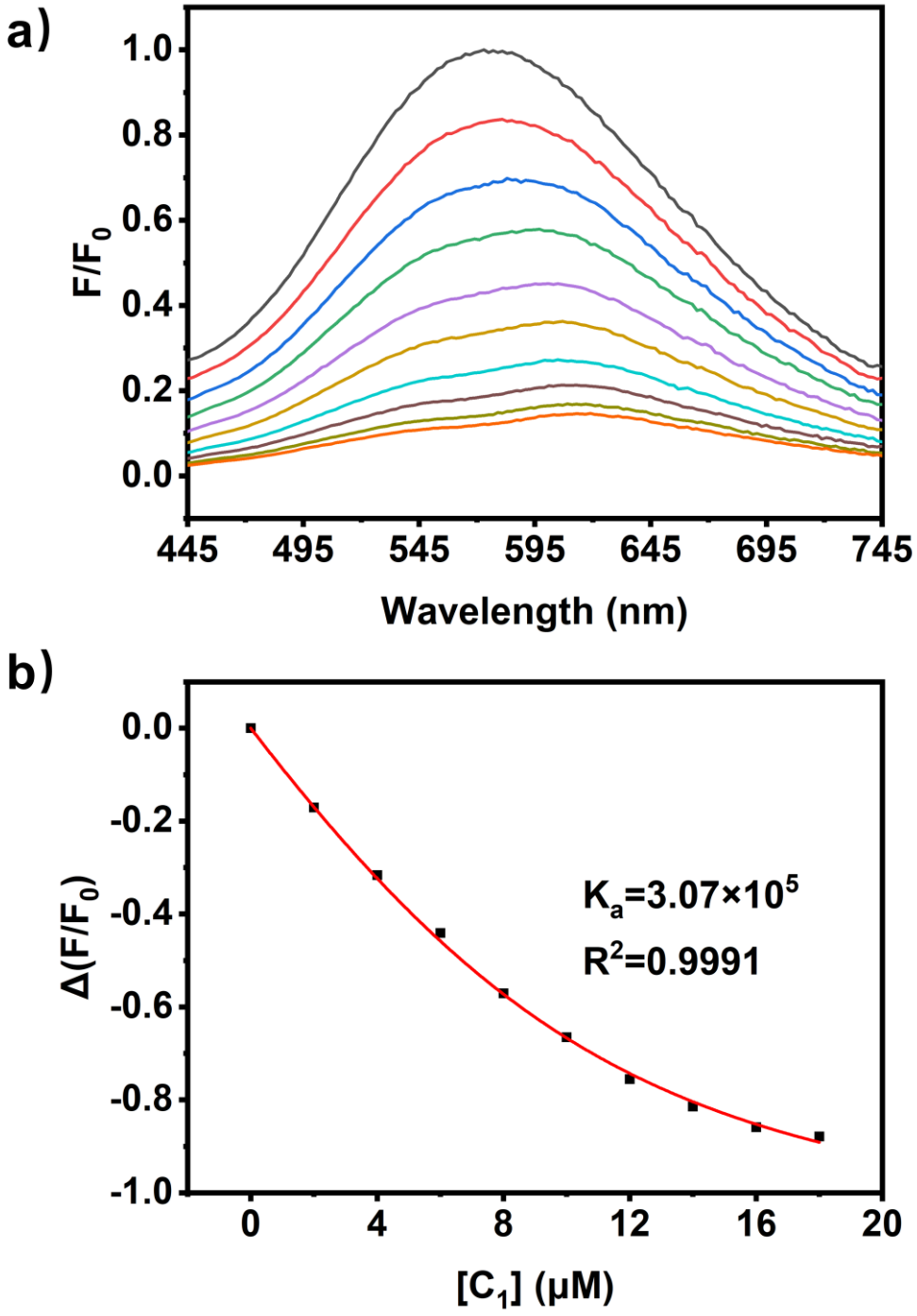

Figure S15. (a) Luminescence spectrum of the AQDS (0.01 mM) upon the addition of **C1** in a DMSO solution. (b) The nonlinear fitting of the titration curve (recorded emission at 573 nm, excitation at 385nm), showing a 1:1 host-guest binding stoichiometry between **C1** and AQDS with an association constant calculated as 3.07 × 10^5 M^{-1}.

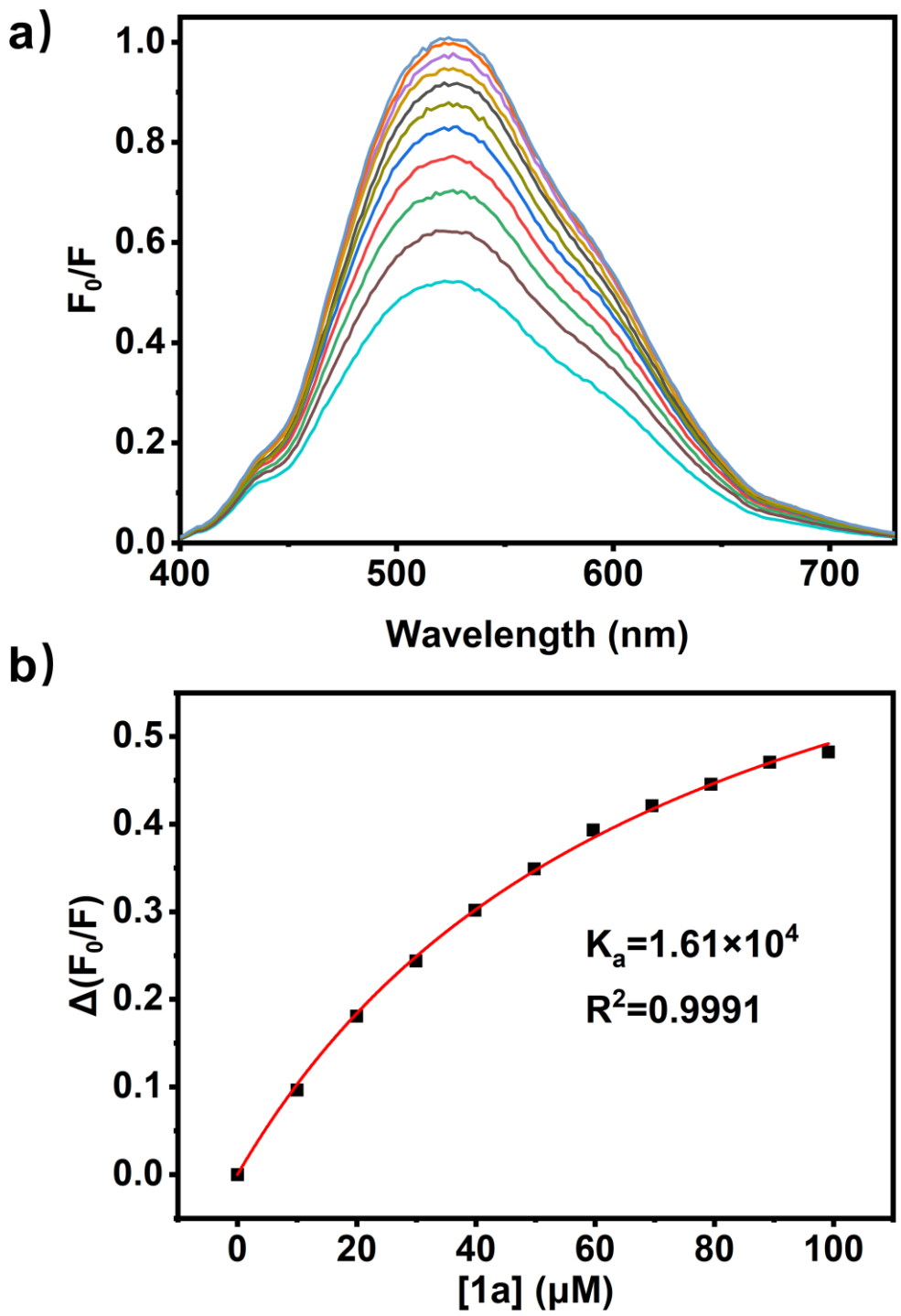

Figure S16. (a) Luminescence spectrum of the $\mathbf{C_1}$ (0.01 mM) upon the addition of **1a** in a DMSO solution. (b) The nonlinear fitting of the titration curve (recorded emission at 525 nm, excitation at 395nm), showing a 1:1 host-guest binding stoichiometry between $\mathbf{C_1}$ and **1a** with an association constant calculated as $1.61 \times 10^4\ M^{-1}$.

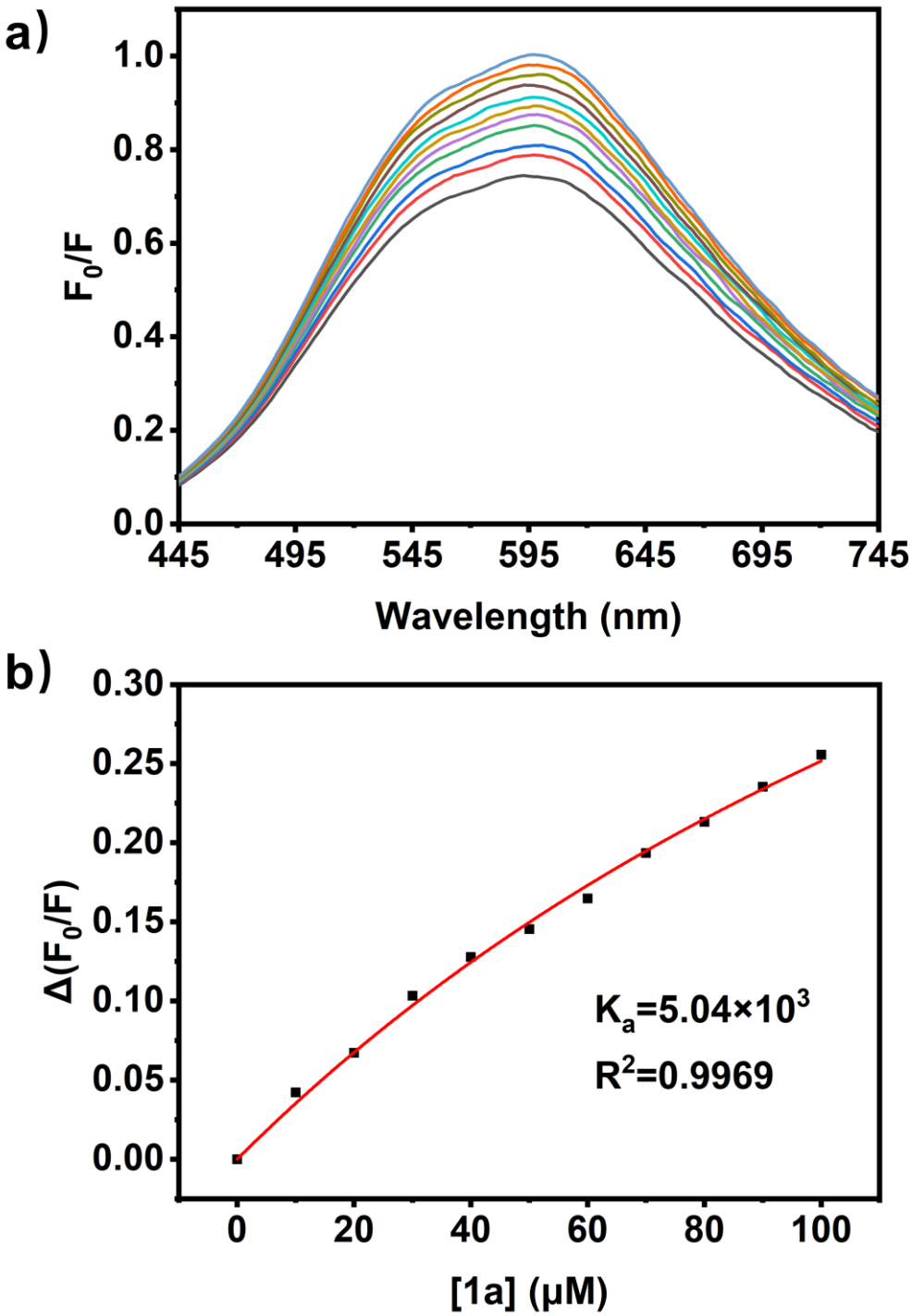

Figure S17. (a) Luminescence spectrum of the $\mathbf{C_{AQ}}$ (0.01 mM) upon the addition of **1a** in a DMSO solution. (b) The nonlinear fitting of the titration curve (recorded emission at 593 nm, excitation at 385nm), showing a 1:1 host-guest binding stoichiometry between $\mathbf{C_{AQ}}$ and **1a** with an association constant calculated as $5.04 \times 10^3\ M^{-1}$.

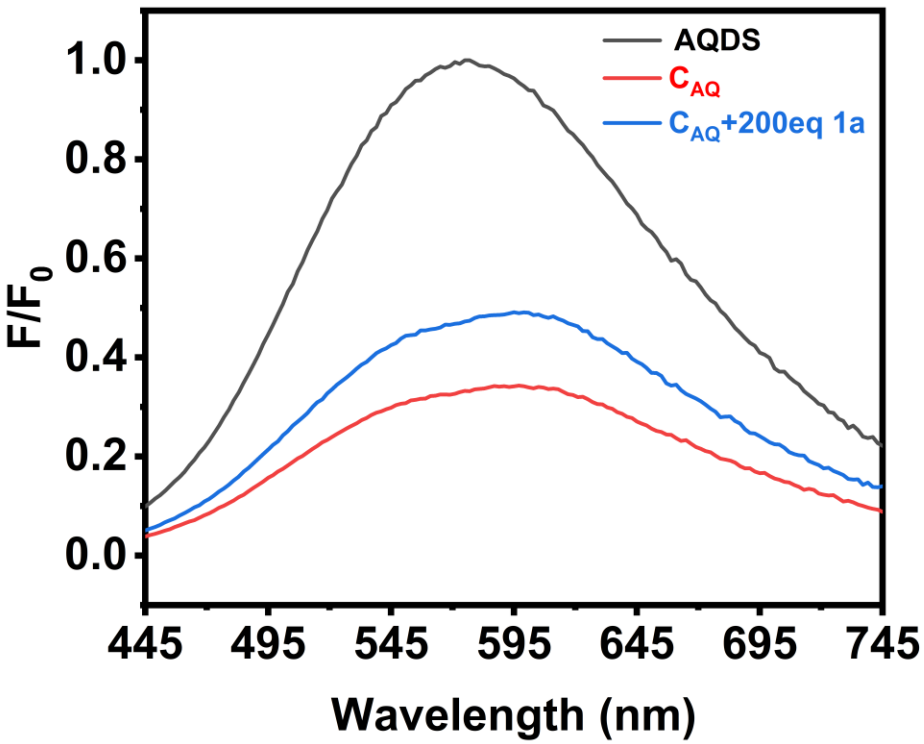

Figure S18. Fluorescence emission spectra of free AQDS (0.01 mM), the $\mathbf{C_{AQ}}$ host-guest complex (0.01 mM), and $\mathbf{C_{AQ}}$ in the presence of 200eq **1a**.

Activated Oxygen Performance.

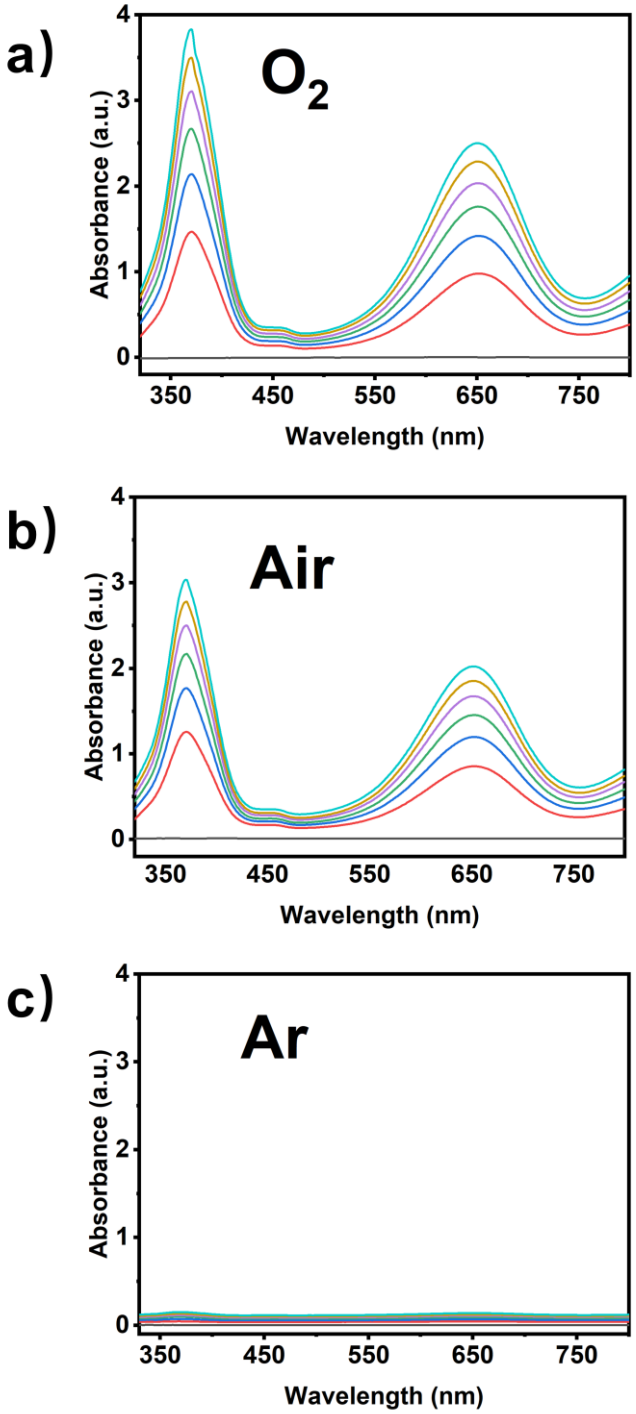

Figure S19. Curves of C_{AQ} oxidation of TMB along with different atmosphere over time. (a) O_2; (b) Air; (c) Ar.

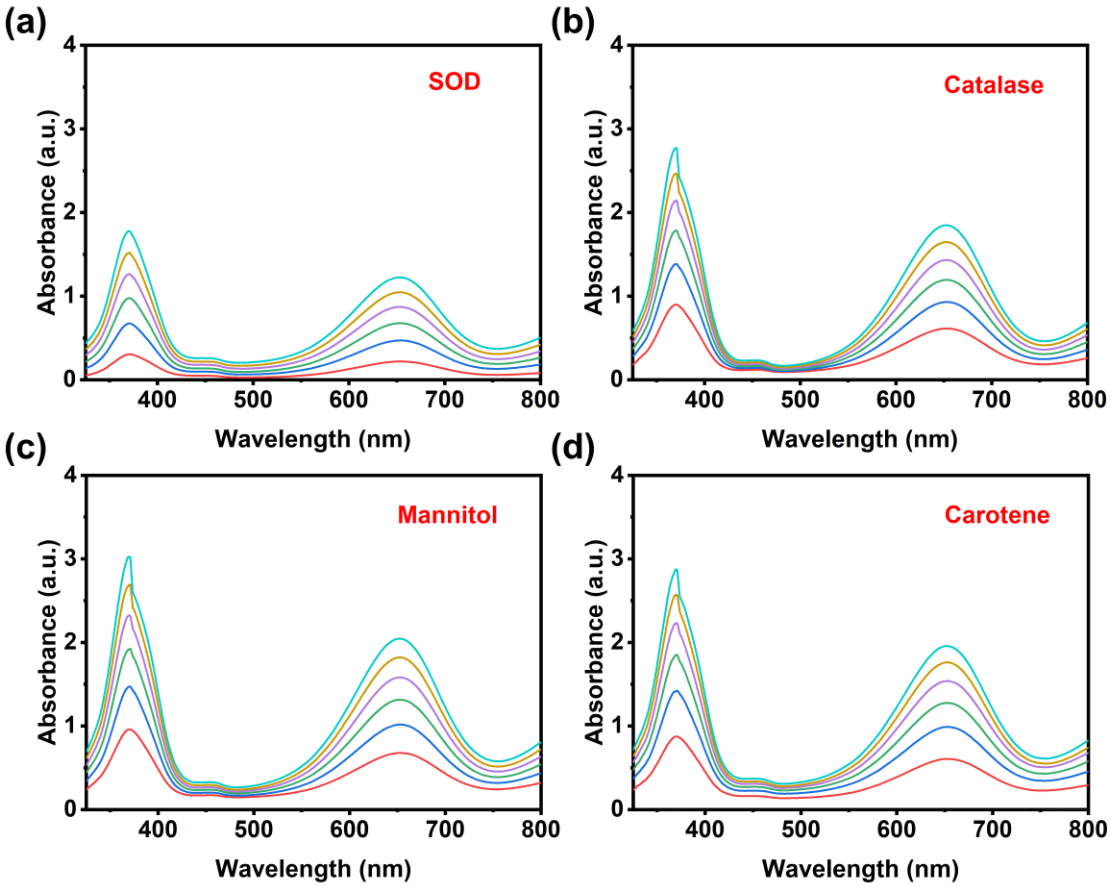

Figure S20. Curves of C_{AQ} oxidation of TMB along with different active oxygen sacrificial agents over time. (a) Superoxide dismutase (SOD); (b) Catalase; (c) Mannitol; (d) Carotene.

HPLC spectra

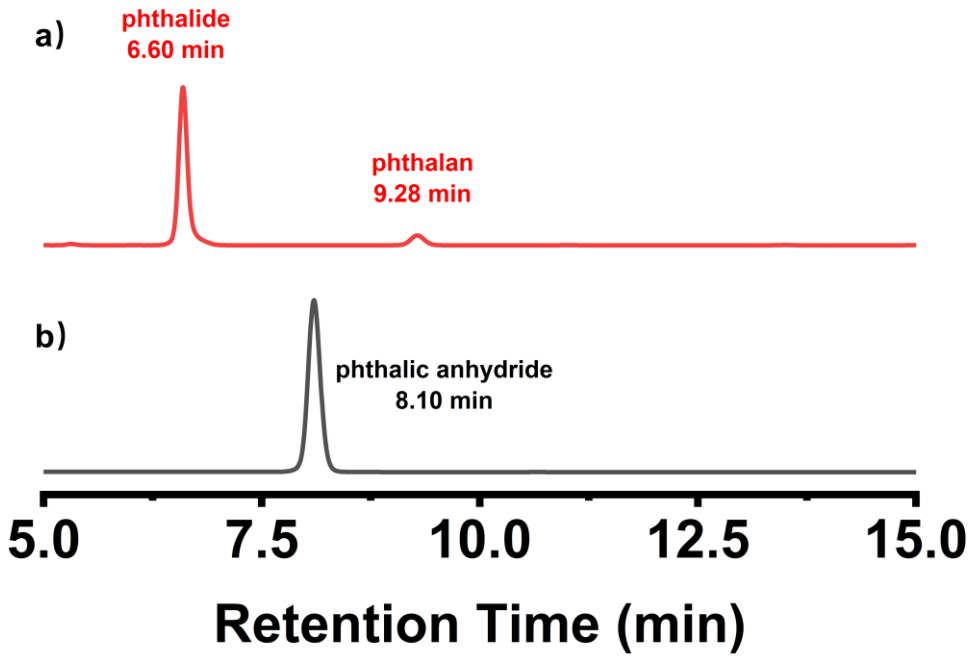

Figure S21. HPLC traces of (a) the reaction filtrate after catalysis and removal of $\mathbf{C_{AQ}}$; (b) authentic phthalic anhydride standard. No characteristic peak of phthalic anhydride was detected, confirming the absence of over-oxidation byproducts.

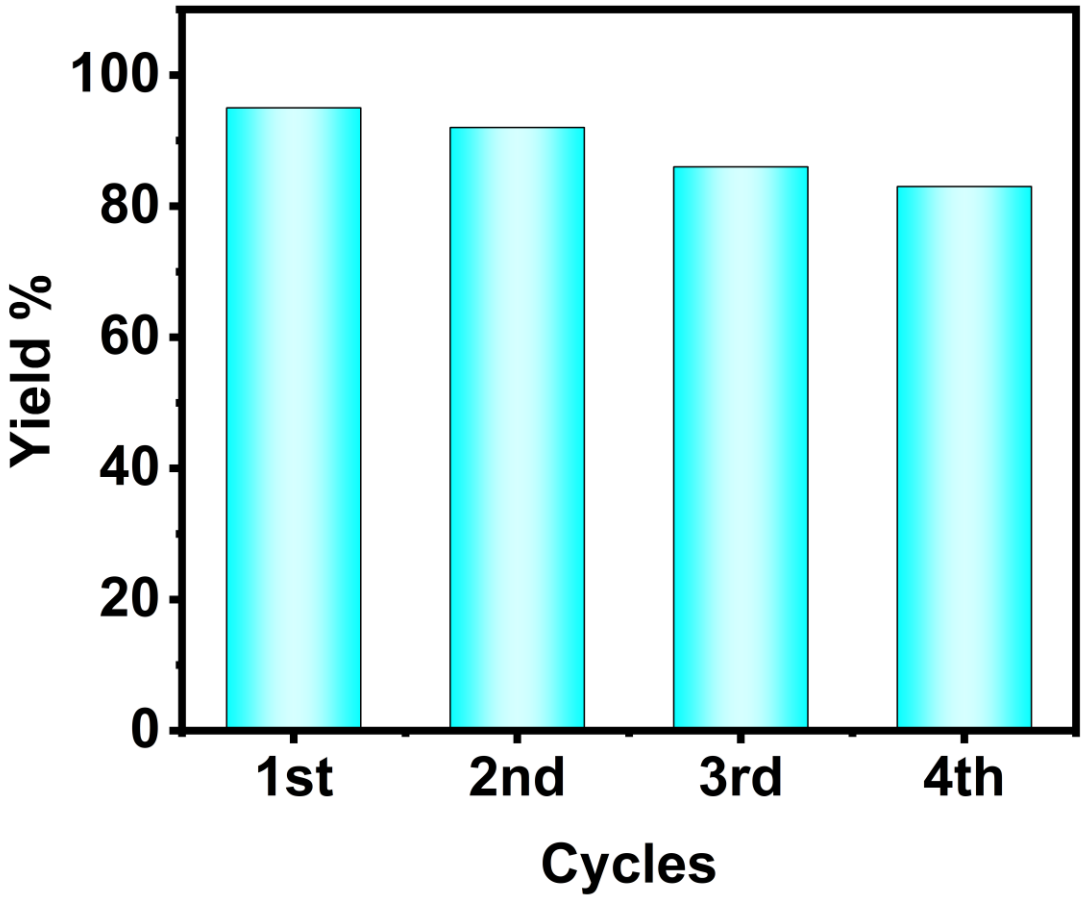

Figure S22. Recycling experiments of the $\mathbf{C_{AQ}}$ catalyst in the photocatalytic oxidation of substrate **1a**. Reaction conditions: **1a** (0.1mmol), $\mathbf{C_{AQ}}$ (0.5 mol%), DMSO/CH_3CN (1:3, 4mL), 395nm LED, O_2, 4h per cycle. The phthalide yield was determined by HPLC analysis using external standard method.

Kinetics experiments

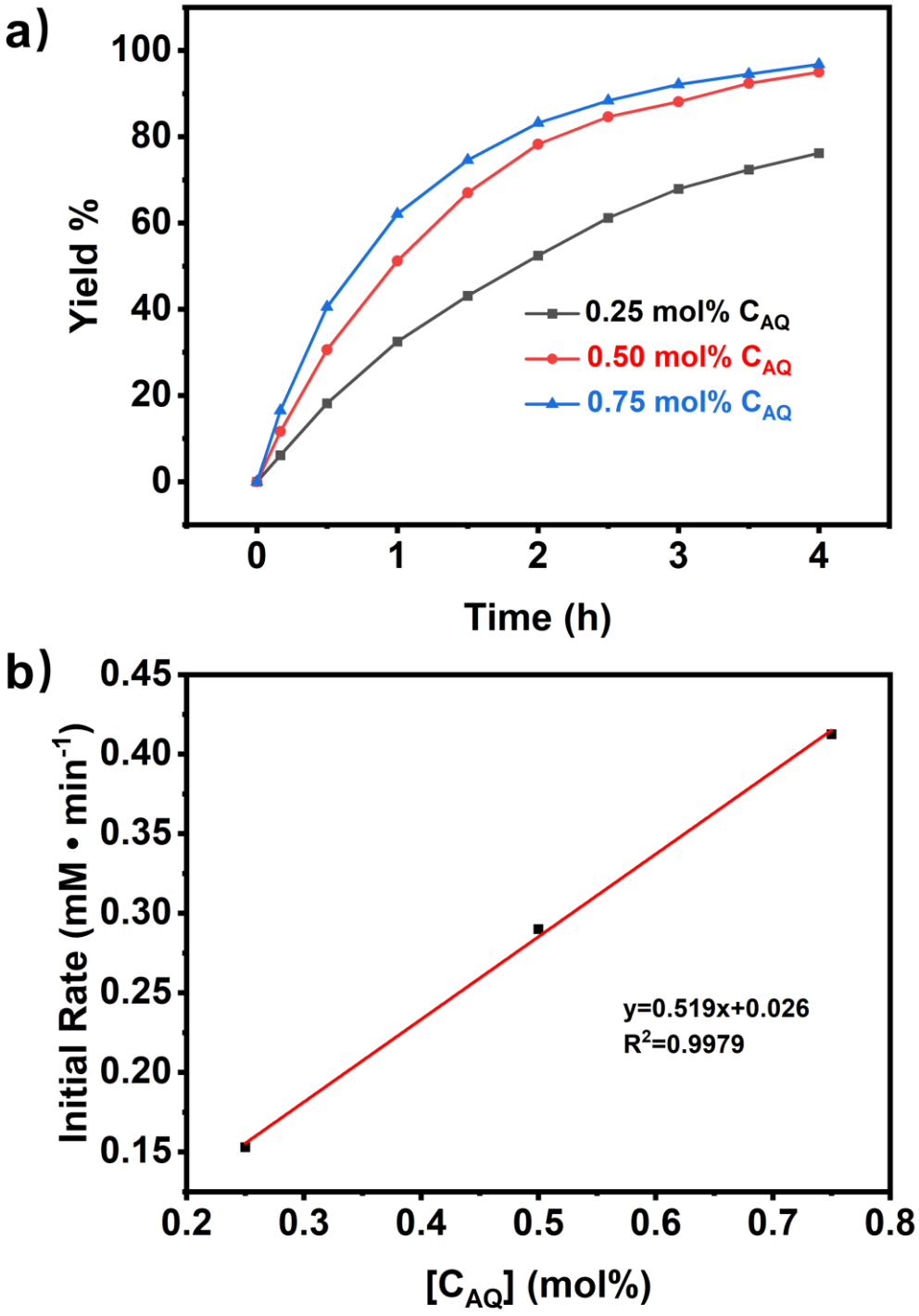

Figure S23. (a) Kinetics experiments of **1a** C(sp^3)-H bonds activation at different C_{AQ} concentrations. (b) Initial rate of reaction as a function of C_{AQ} concentration.

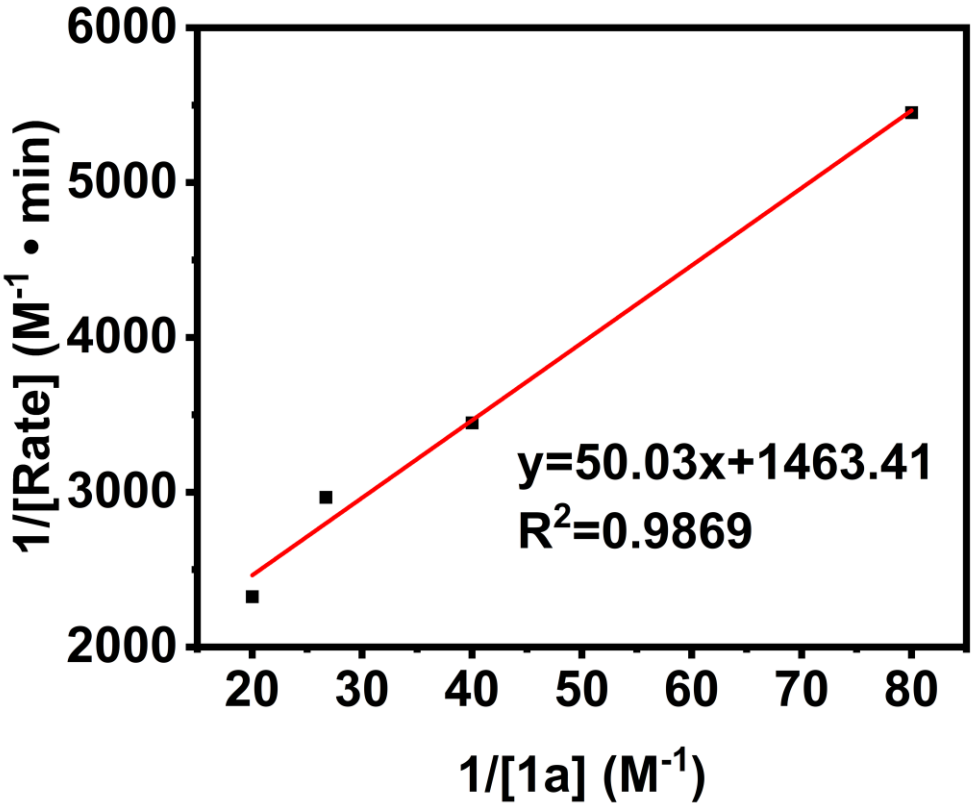

Figure S24. The Lineweaver-Burk double-reciprocal plot of initial reaction rate versus the concentration of the **1a**, indicating that the catalytic process follows a Michaelis-Menten kinetic mechanism.

4. Characterization Data for All Compounds

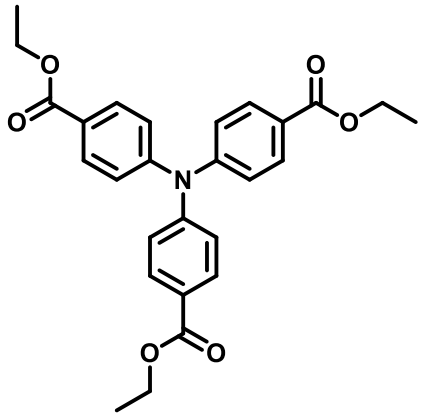

^{1}H NMR (500 MHz, $CDCl_3$) δ 7.98 (d, *J* = 7.6 Hz, 3H), 7.15 (d, *J* = 7.6 Hz, 3H), 4.39 (q, *J* = 7.1 Hz, 3H), 1.41 (t, *J* = 7.1 Hz, 6H).

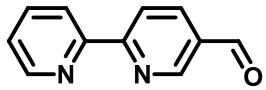

^{1}H NMR (500 MHz, $CDCl_3$) δ 10.19 (s, 1H), 9.15 (d, *J* = 1.2 Hz, 1H), 8.75 (d, *J* = 4.0 Hz, 1H), 8.64 (d, *J* = 8.2 Hz, 1H), 8.53 (d, *J* = 7.9 Hz, 1H), 8.31 (d, *J* = 6.1 Hz, 1H), 7.92-7.87 (m, 1H), 7.43-7.39 (m, 1H).

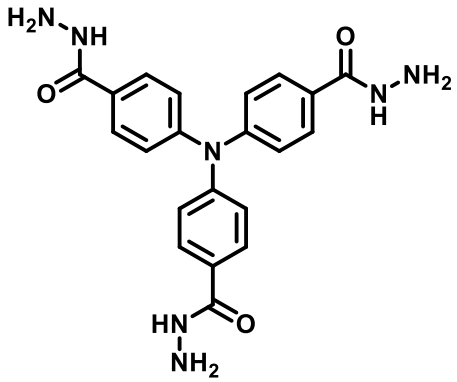

^{1}H NMR (500 MHz, DMSO-d_6) δ 9.69 (s, 3H), 7.79 (d, *J* = 8.7 Hz, 6H), 7.06 (d, *J* = 8.7 Hz, 6H), 4.46 (s, 6H).

L_1

^{1}H NMR (500 MHz, DMSO-d_6) δ 12.10 (s, 3H), 8.97 (s, 3H), 8.73 (d, *J* = 6.1 Hz, 3H), 8.58 (s, 3H), 8.50 (d, *J* = 8.4 Hz, 3H), 8.44 (d, *J* = 7.9 Hz, 3H), 8.33 (d, *J* = 10.4 Hz, 3H), 7.98 (d, *J* = 8.9 Hz, 9H), 7.52-7.48 (m, 3H), 7.26 (d, *J* = 8.7 Hz, 6H).

L_2

^{1}H NMR (500 MHz, DMSO-d_6) δ 11.78 (s, 1H), 8.94 (d, J = 2.2 Hz, 1H), 8.72 (d, J = 4.8 Hz, 1H), 8.54 (s, 1H), 8.49 (d, J = 8.3 Hz, 1H), 8.44 (d, J = 7.9 Hz, 1H), 8.28 (d, J = 8.3 Hz, 1H), 8.01 – 7.95 (m, 1H), 7.85 (d, J = 9.0 Hz, 2H), 7.52 – 7.46 (m, 1H), 6.78 (d, J = 9.1 Hz, 2H), 3.02 (s, 6H).

C_1

^{1}H NMR (500 MHz, DMSO-d$_6$) δ 12.14 (s, 3H), 8.90 (t, *J* = 9.2 Hz, 6H), 8.54 (d, *J* = 9.3 Hz, 3H), 8.30 (d, *J* = 7.5 Hz, 3H), 8.13 (s, 3H), 7.74 (d, *J* = 8.9 Hz, 6H), 7.63 (d, *J* = 6.6 Hz, 3H), 7.43 (d, *J* = 6.4 Hz, 3H), 7.30 (s, 3H), 7.10 (d, *J* = 8.9 Hz, 6H).

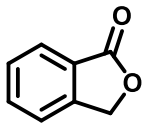

(2a)^{1}H NMR (500 MHz, CDCl$_3$) δ 7.95 (d, *J* = 7.6 Hz, 1H), 7.74-7.68 (m, 1H), 7.56 (t, *J* = 7.2 Hz, 1H), 7.52 (d, *J* = 7.8 Hz, 1H), 5.35 (s, 2H).

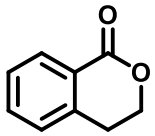

(2b) ^{1}H NMR (500 MHz, DMSO-d$_6$) δ 7.93 (d, *J* = 11.7 Hz, 1H), 7.69-7.57 (m, 1H), 7.44 (d, *J* = 7.9 Hz, 1H), 7.41 (d, *J* = 6.3 Hz, 1H), 4.54-4.43 (m, 2H), 3.06 (t, *J* = 7.4 Hz, 2H).

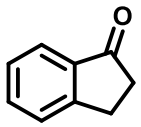

(2c) ^{1}H NMR (500 MHz, CDCl$_3$) δ 7.78 (d, *J* = 7.7 Hz, 1H), 7.64-7.58 (m, 1H), 7.50 (d, *J* = 7.8 Hz, 1H), 7.39 (t, *J* = 7.9 Hz, 1H), 3.19-3.15 (m, 2H), 2.74-2.69 (m, 2H).

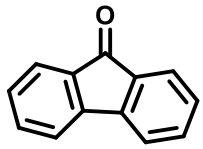

(2d) ^{1}H NMR (500 MHz, CDCl$_3$) δ 7.67 (d, *J* = 7.3 Hz, 2H), 7.53 (d, *J* = 7.3 Hz, 2H), 7.51 – 7.47 (m, 2H), 7.33 – 7.29 (m, 2H).

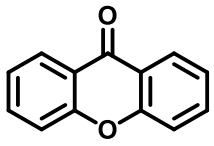

(2e) ^{1}H NMR (500 MHz, CDCl$_3$) δ 8.36 (d, *J* = 9.8 Hz, 2H), 7.74 (t, *J* = 6.9 Hz, 2H), 7.51 (d, *J* = 8.4 Hz, 2H), 7.40 (t, *J* = 8.1 Hz, 2H).

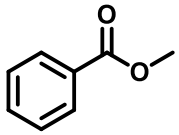

(2f)^{1}H NMR (500 MHz, CDCl$_3$) δ 8.05 (d, *J* = 7.1 Hz, 2H), 7.56 (t, *J* = 7.5 Hz, 1H), 7.44 (t, *J* = 7.6 Hz, 2H), 3.92 (s, 3H).

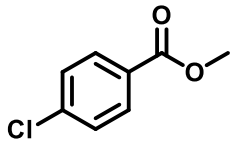

(2g)^{1}H NMR (500 MHz, $CDCl_3$) δ 8.00 (d, *J* = 8.7 Hz, 2H), 7.43 (d, *J* = 8.7 Hz, 2H), 3.94 (s, 3H).

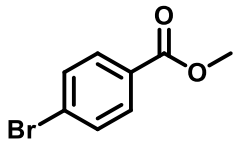

(2h)^{1}H NMR (500 MHz, $CDCl_3$) δ 7.90 (d, *J* = 8.7 Hz, 2H), 7.59 (d, *J* = 8.7 Hz, 2H), 3.92 (s, 3H).

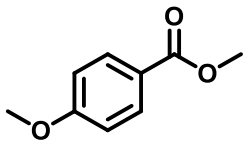

(2i)^{1}H NMR (500 MHz, $CDCl_3$) δ 8.02 (d, *J* = 9.0 Hz, 2H), 6.94 (d, *J* = 9.0 Hz, 2H), 3.91 (s, 3H), 3.88 (s, 3H).

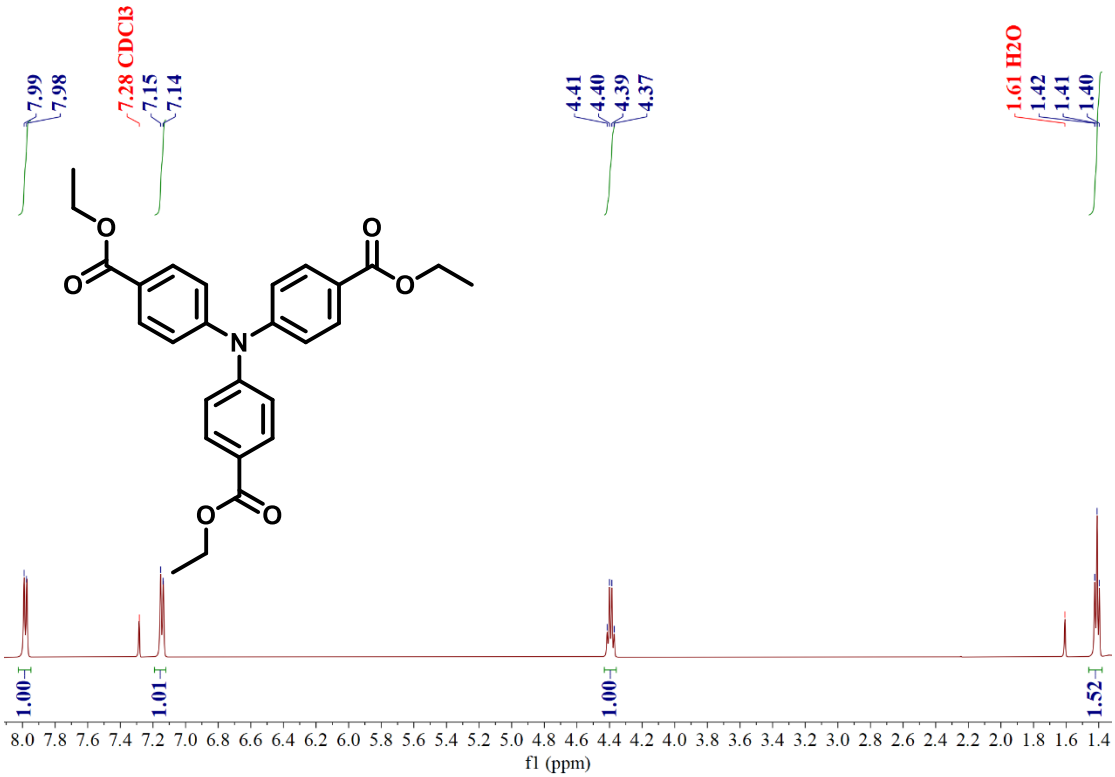
7.99
7.98
7.28 CDCl3
7.15
7.14
4.41
4.40
4.39
4.37
1.61 H2O
1.42
1.41
1.40
1.00
1.01
1.00
1.52
f1 (ppm)

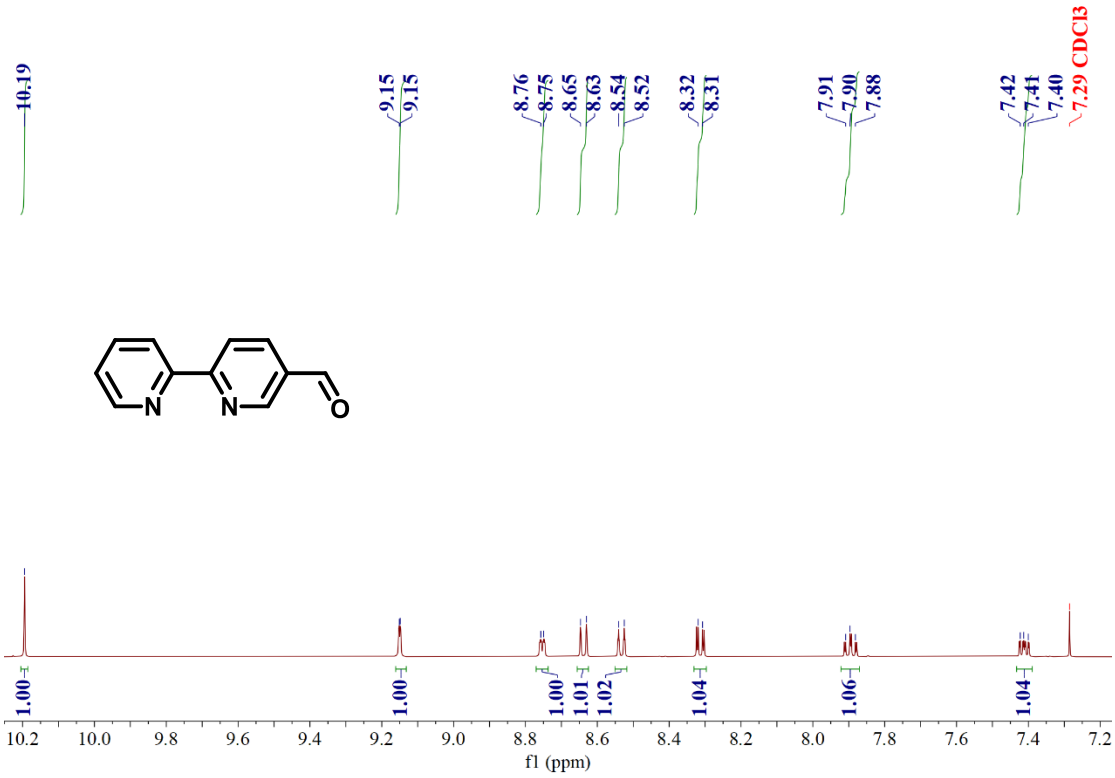
10.19
9.15
9.15
8.76
8.75
8.65
8.63
8.54
8.52
8.32
8.31
7.91
7.90
7.88
7.42
7.41
7.40
7.29 CDCl3
1.00
1.00
1.00
1.01
1.02
1.04
1.06
1.04
f1 (ppm)

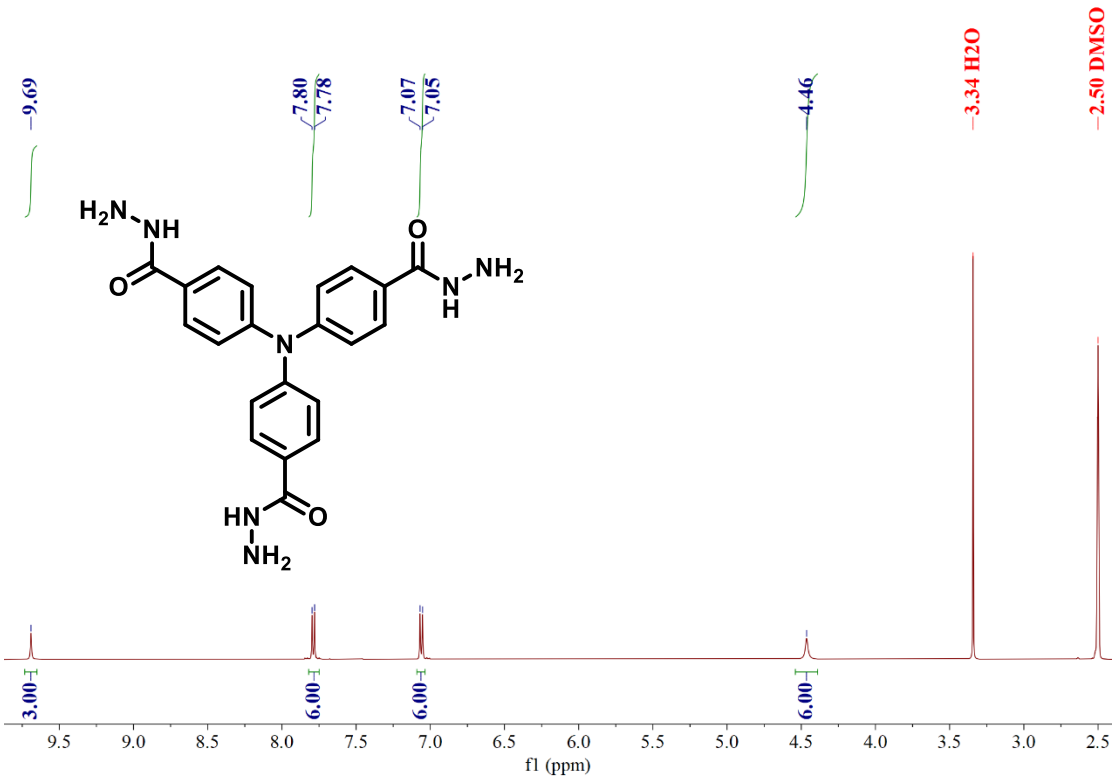
9.69
7.80
7.78
7.07
7.05
4.46
3.34 H2O
2.50 DMSO
3.00
6.00
6.00
6.00
f1 (ppm)

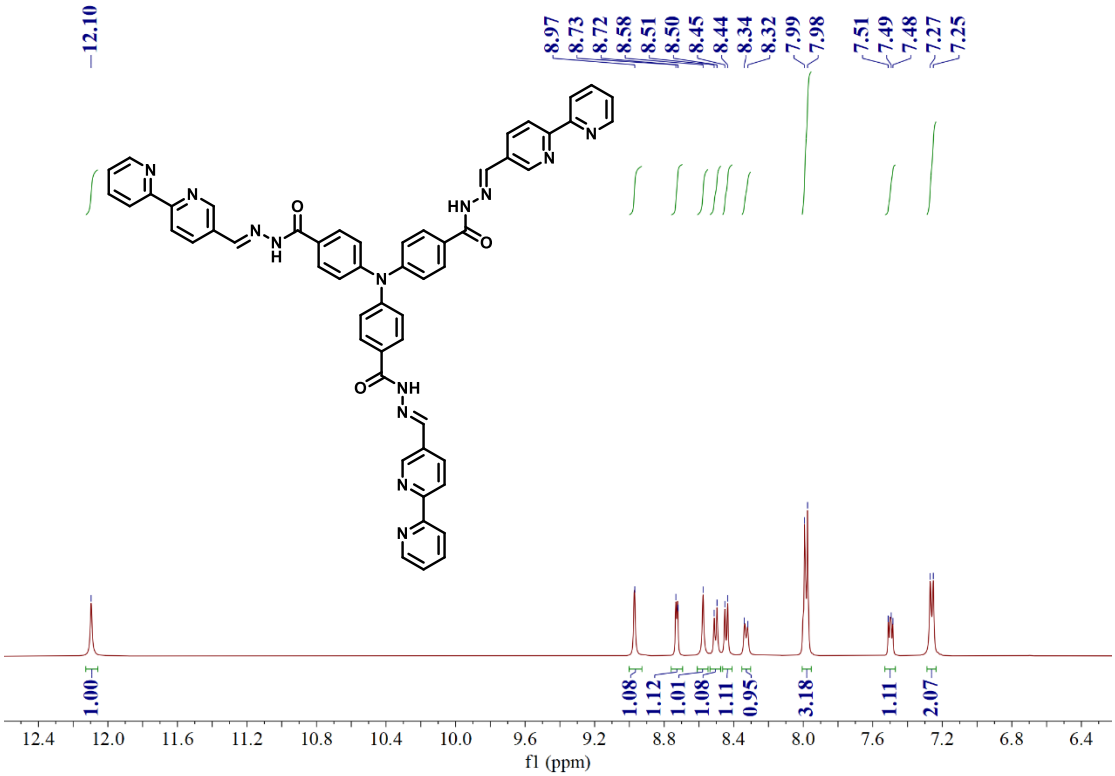
12.10
8.97
8.73
8.72
8.58
8.51
8.50
8.45
8.44
8.34
8.32
7.99
7.98
7.51
7.49
7.48
7.27
7.25
1.00
1.08
1.12
1.01
1.08
1.11
0.95
3.18
1.11
2.07
f1 (ppm)

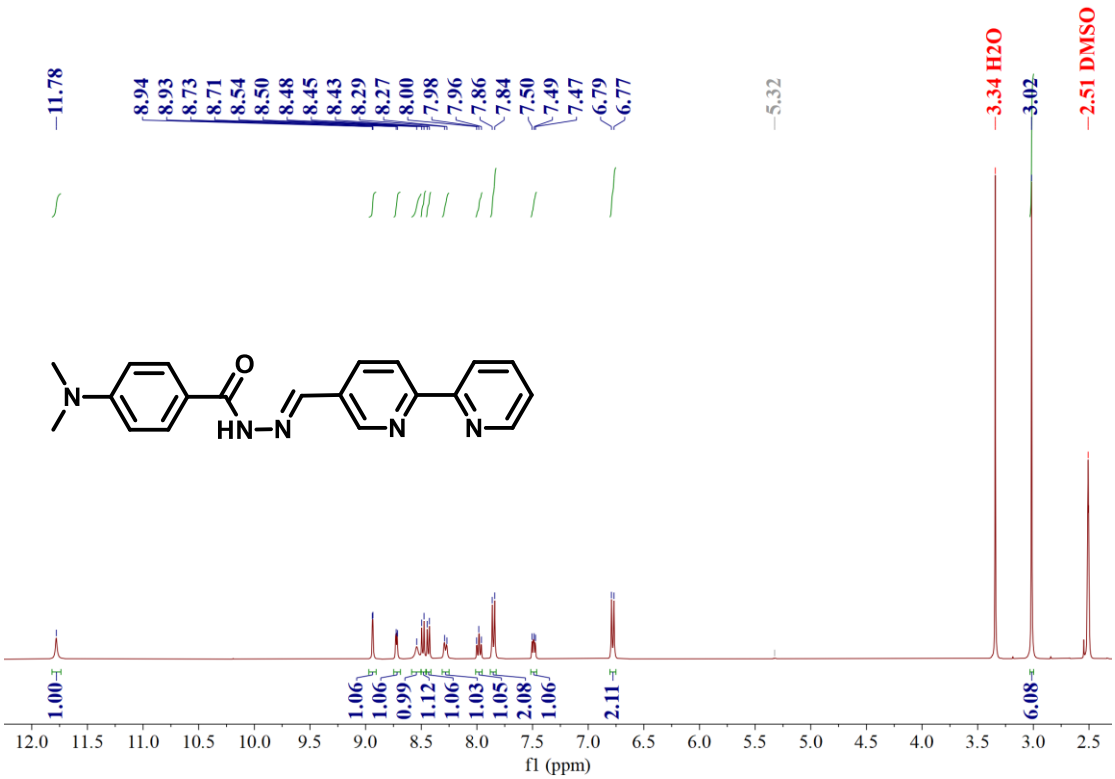
11.78
8.94
8.93
8.73
8.71
8.54
8.50
8.48
8.45
8.43
8.29
8.27
8.00
7.98
7.96
7.86
7.84
7.50
7.49
7.47
6.79
6.77
5.32
3.34 H2O
3.02
2.51 DMSO
O
HN–N
N
N
1.00
1.06
1.06
0.99
1.12
1.06
1.03
1.05
2.08
1.06
2.11
6.08
f1 (ppm)

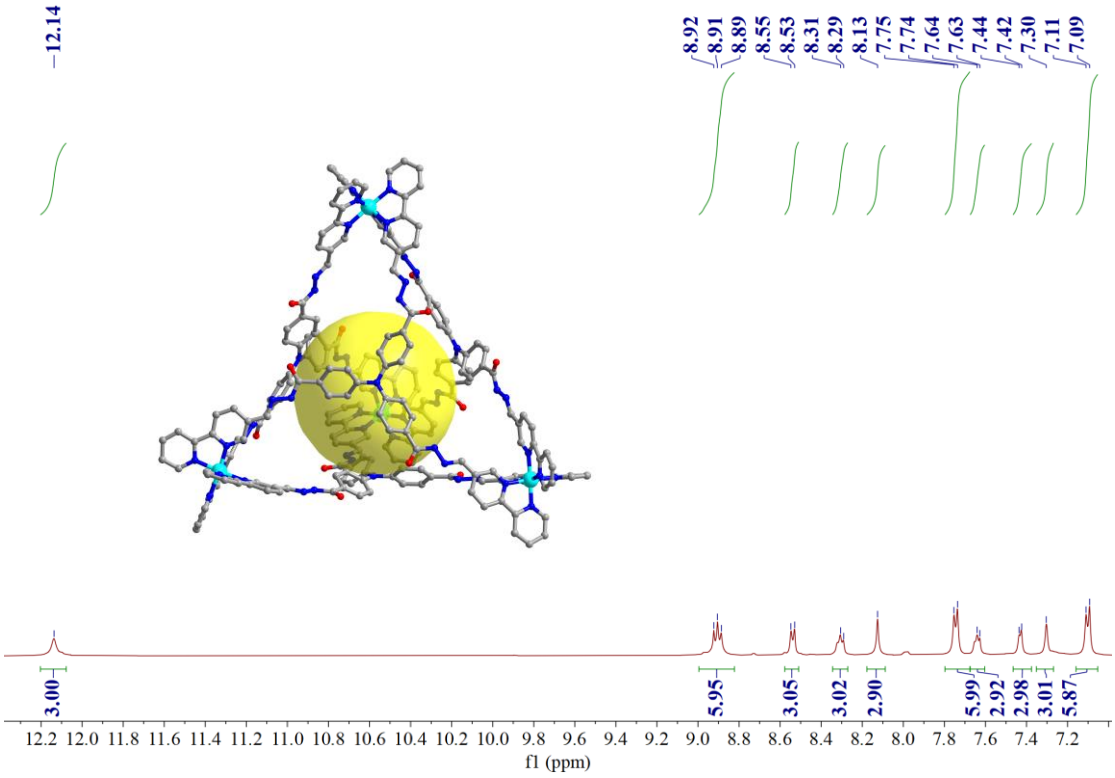
12.14
8.92
8.91
8.89
8.55
8.53
8.31
8.29
8.13
7.75
7.74
7.64
7.63
7.44
7.42
7.30
7.11
7.09
3.00
5.95
3.05
3.02
2.90
5.99
2.92
2.98
3.01
5.87
f1 (ppm)

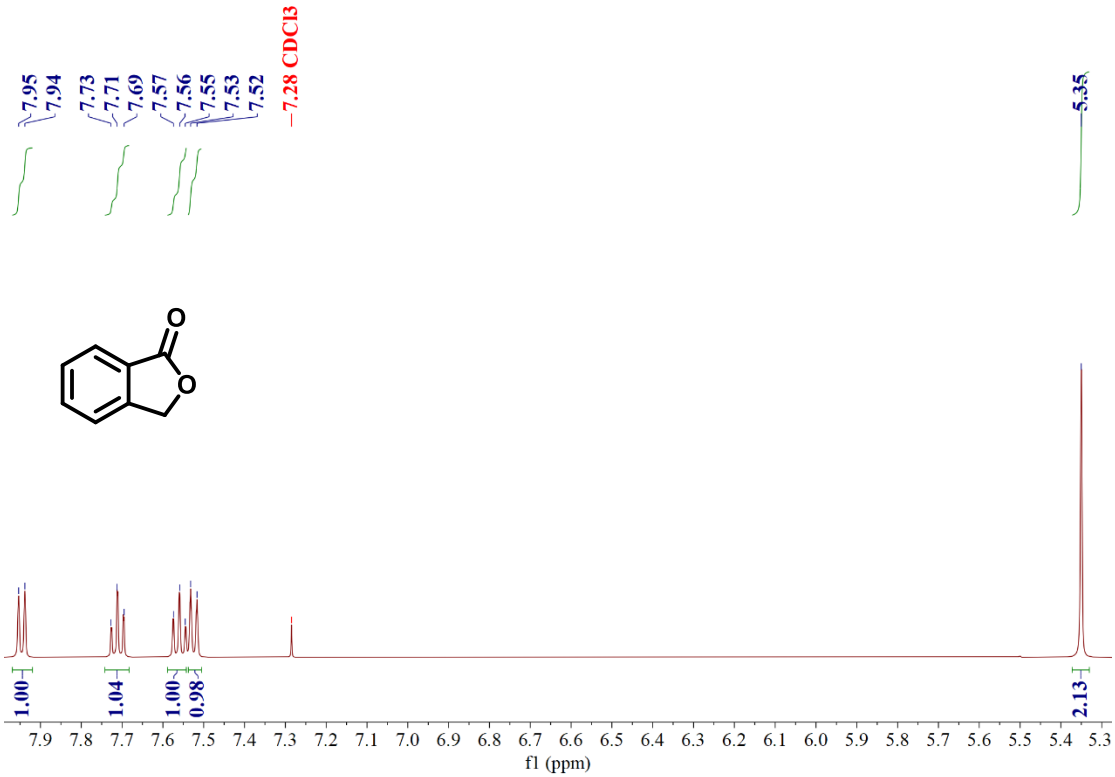
7.95
7.94
7.73
7.71
7.69
7.57
7.56
7.55
7.53
7.52
7.28 CDCl3
5.35
1.00
1.04
1.00
0.98
2.13
f1 (ppm)

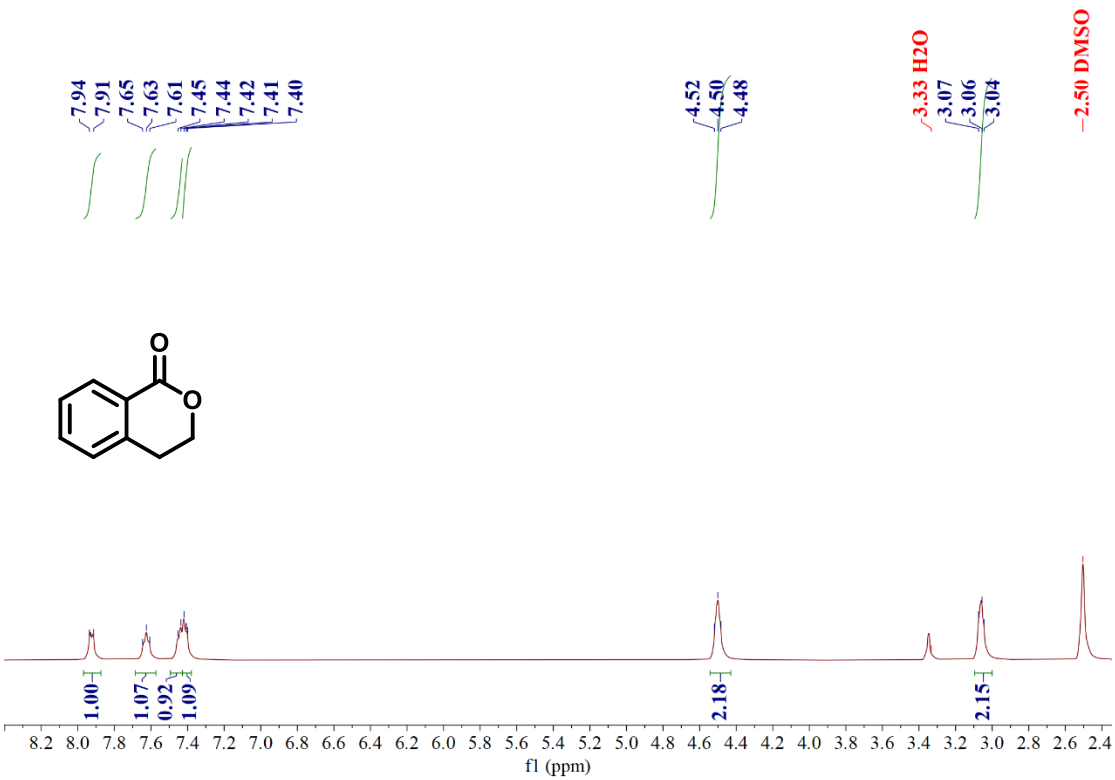
7.94
7.91
7.65
7.63
7.61
7.45
7.44
7.42
7.41
7.40
4.52
4.50
4.48
3.33 H2O
3.07
3.06
3.04
2.50 DMSO
1.00
1.07
0.92
1.09
2.18
2.15
f1 (ppm)

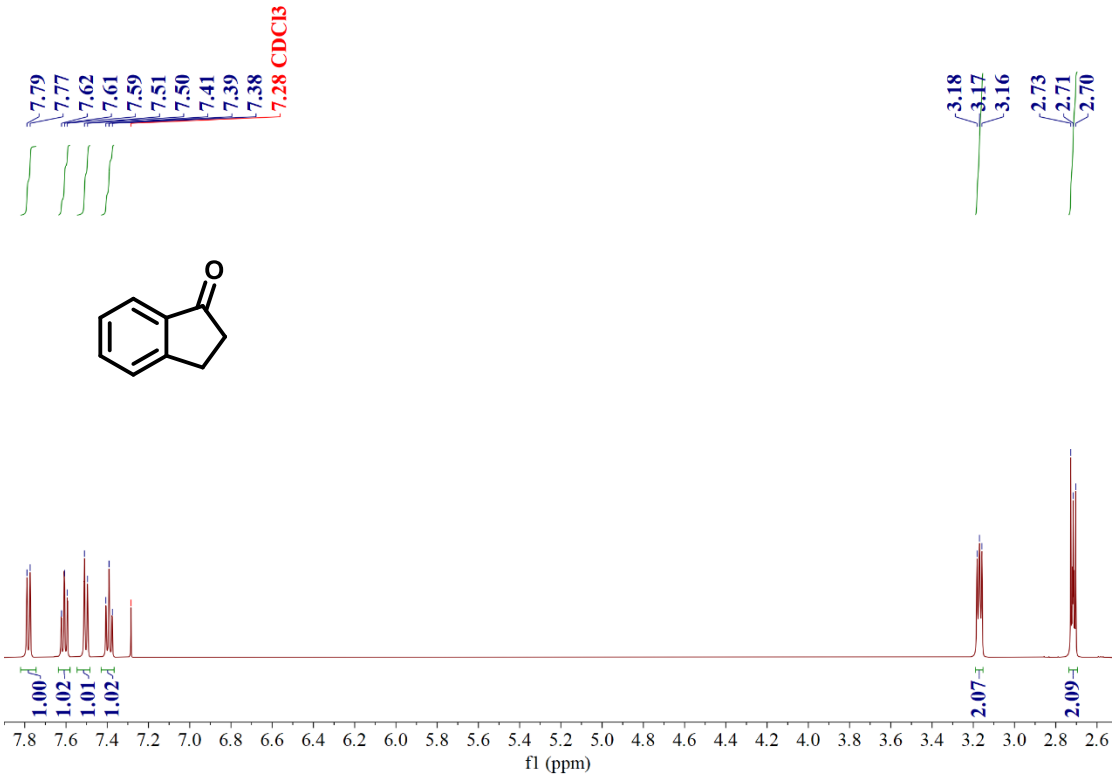
7.79
7.77
7.62
7.61
7.59
7.51
7.50
7.41
7.39
7.38
7.28 CDCl3
3.18
3.17
3.16
2.73
2.71
2.70
O
1.00
1.02
1.01
1.02
2.07
2.09
7.8 7.6 7.4 7.2 7.0 6.8 6.6 6.4 6.2 6.0 5.8 5.6 5.4 5.2 5.0 4.8 4.6 4.4 4.2 4.0 3.8 3.6 3.4 3.2 3.0 2.8 2.6
f1 (ppm)

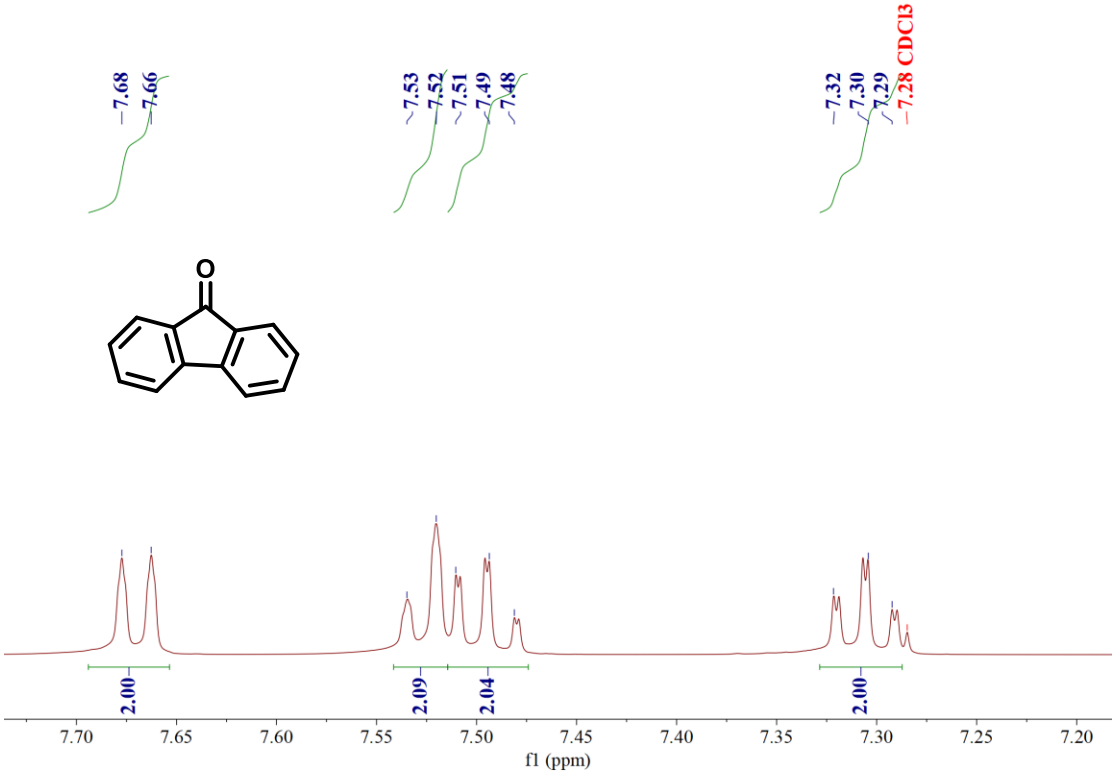
7.68
7.66
7.53
7.52
7.51
7.49
7.48
7.32
7.30
7.29
7.28 CDCl3
O
2.00
2.09
2.04
2.00
7.70 7.65 7.60 7.55 7.50 7.45 7.40 7.35 7.30 7.25 7.20
f1 (ppm)

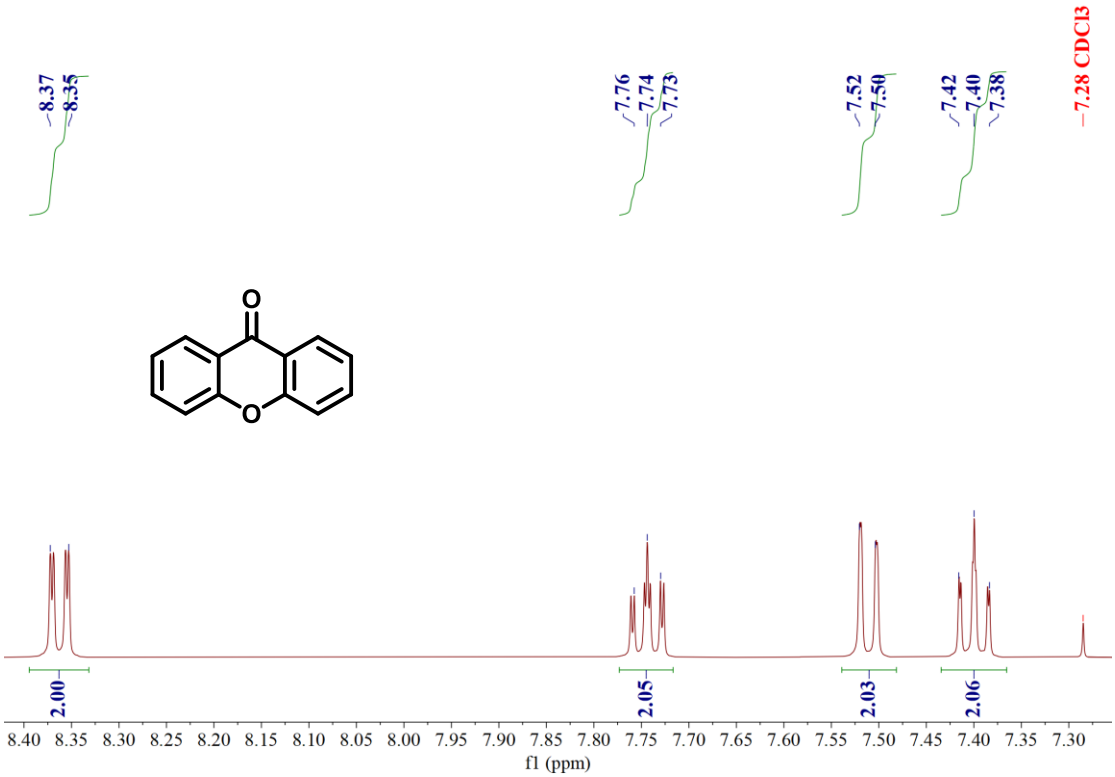
8.37
8.35
7.76
7.74
7.73
7.52
7.50
7.42
7.40
7.38
7.28 CDCl3
O
O
2.00
2.05
2.03
2.06
8.40 8.35 8.30 8.25 8.20 8.15 8.10 8.05 8.00 7.95 7.90 7.85 7.80 7.75 7.70 7.65 7.60 7.55 7.50 7.45 7.40 7.35 7.30
f1 (ppm)

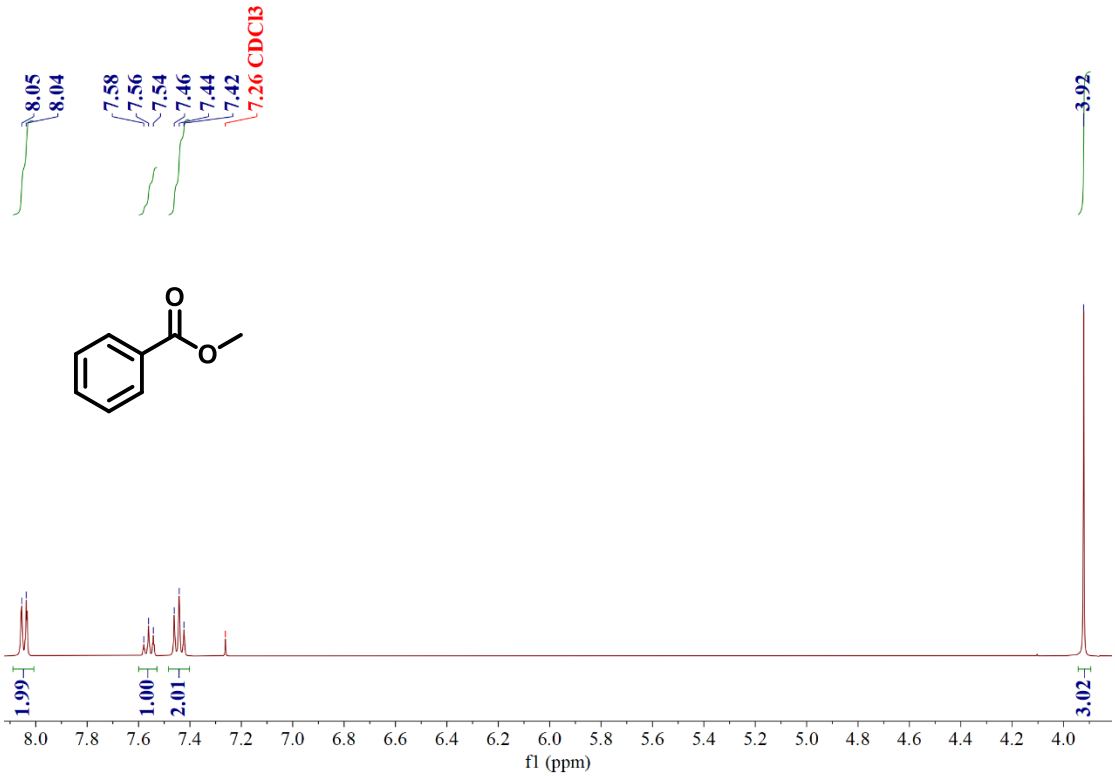
8.05
8.04
7.58
7.56
7.54
7.46
7.44
7.42
7.26 CDCl3
3.92
O
O
1.99
1.00
2.01
3.02
8.0 7.8 7.6 7.4 7.2 7.0 6.8 6.6 6.4 6.2 6.0 5.8 5.6 5.4 5.2 5.0 4.8 4.6 4.4 4.2 4.0
f1 (ppm)

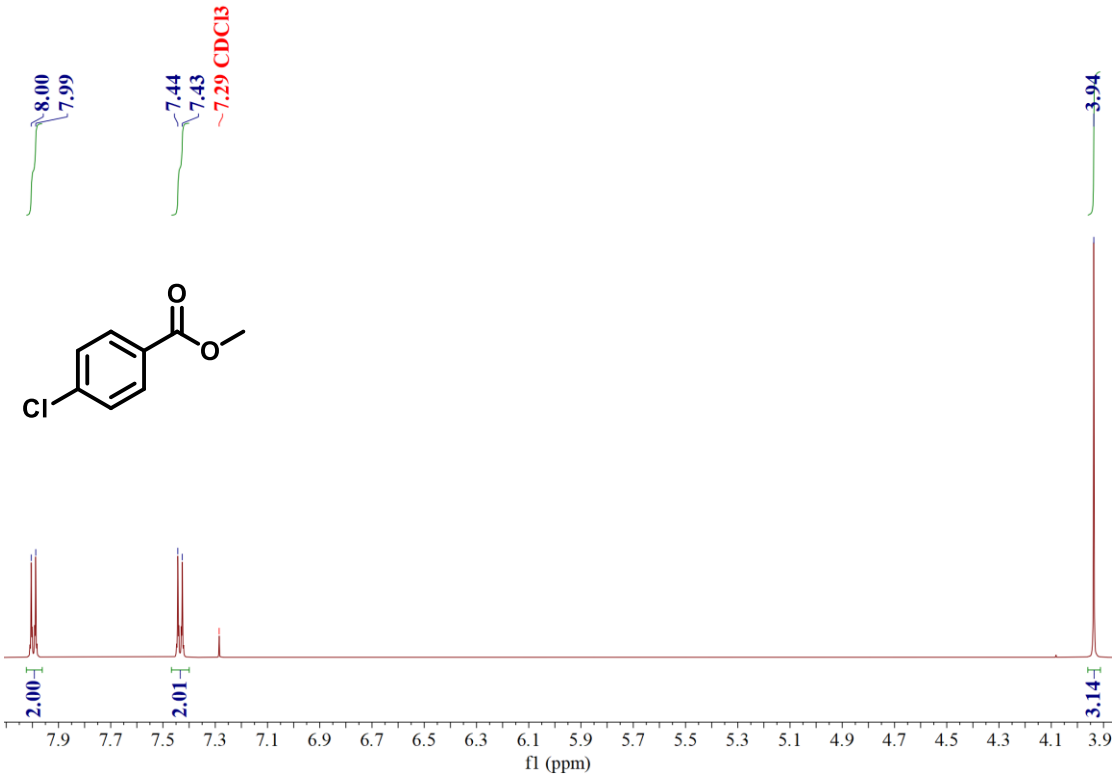
8.00
7.99
7.44
7.43
7.29 CDCl3
3.94
O
O
Cl
2.00
2.01
3.14
7.9 7.7 7.5 7.3 7.1 6.9 6.7 6.5 6.3 6.1 5.9 5.7 5.5 5.3 5.1 4.9 4.7 4.5 4.3 4.1 3.9
f1 (ppm)

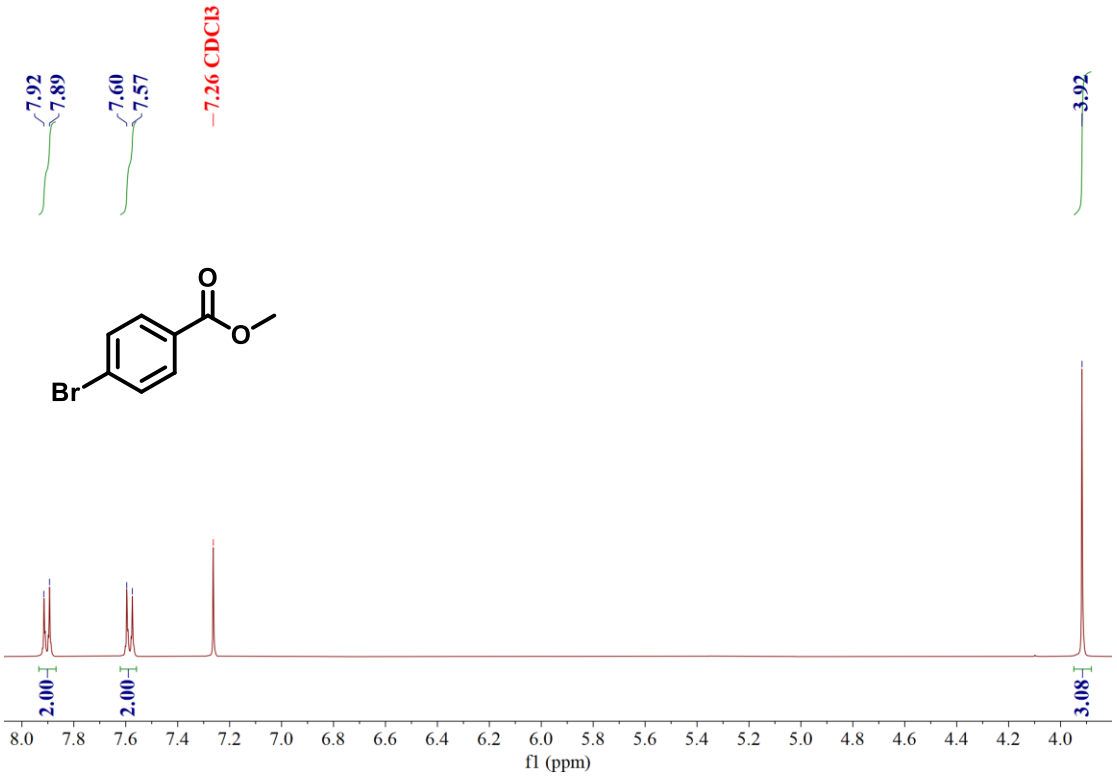
7.92
7.89
7.60
7.57
7.26 CDCl3
3.92
O
O
Br
2.00
2.00
3.08
8.0 7.8 7.6 7.4 7.2 7.0 6.8 6.6 6.4 6.2 6.0 5.8 5.6 5.4 5.2 5.0 4.8 4.6 4.4 4.2 4.0
f1 (ppm)

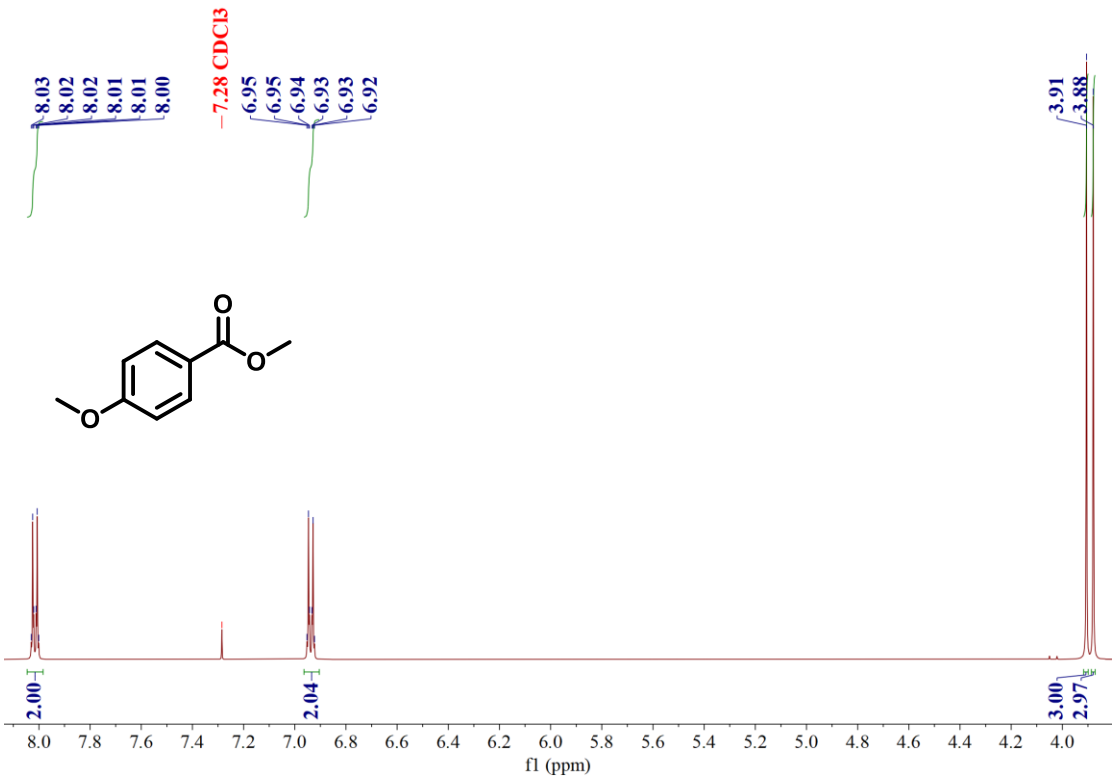
8.03
8.02
8.02
8.01
8.01
8.00
7.28 CDCl3
6.95
6.95
6.94
6.93
6.93
6.92
3.91
3.88
O
O
O
2.00
2.04
3.00
2.97
8.0 7.8 7.6 7.4 7.2 7.0 6.8 6.6 6.4 6.2 6.0 5.8 5.6 5.4 5.2 5.0 4.8 4.6 4.4 4.2 4.0
f1 (ppm)

References

1. J. Wang; C. He; P. Wu; J. W and C. Duan, J. Am. Chem. Soc., 2011, 32, 12402-12405.
2. J.-W. Zhu, H.-D. Ou, N. W. Xu, W. Deng and Z.-J. Yao, Dyes Pigm., 2020, 176, 108196.
3. J. Wei, L. Zhao, Y. Zhang, G. Han, C. He, C. Wang and C. Duan, J. Am. Chem. Soc., 2023, 145, 6719–6729.
4. SMART, Data collection software (version 5.629) (Bruker AXS Inc.; Madison, WI, 2003).
5. SAINT, Data reduction software (version 6.45) (Bruker AXS Inc.; Madison, WI, 2003).
6. Sheldrick, G. SHELXTL97, Program for Crystal Structure Solution (University of Göttingen: Göttingen, Germany, 1997).
7. Spek, A. L. Single-crystal structure validation with the program PLATON. J. Appl. Cryst. 36, 7-13 (2003).